
MapFormer: Self-Supervised Learning of Cognitive Maps with *Input-Dependent* Positional Embeddings

Victor Rambaud^{1,2} Salvador Mascarenhas¹

Yair Lakretz²

¹Institut Jean Nicod

²Laboratoire de Sciences Cognitives et Psycholinguistique (LSCP)

Département d’Études Cognitives

École Normale Supérieure, EHESS, CNRS, PSL University

Abstract

A cognitive map is an internal model which encodes the abstract relationships among entities in the world, giving humans and animals the flexibility to adapt to new situations, with a strong out-of-distribution (OOD) generalization that current AI systems still do not possess. To bridge this gap, we introduce *MapFormers*, new architectures based on Transformer models, which can learn cognitive maps from observational data and perform path integration in parallel, in a self-supervised manner. Cognitive maps are learned in the model by disentangling structural relationships in the inputs from their specific content, a property that can be achieved naturally by updating the positional encoding in Transformers with input-dependent matrices. We developed two variants of *MapFormers* that unify absolute and relative positional encoding to model episodic (EM) and working memory (WM), respectively. We tested *MapFormers* on several tasks, including a classic 2D navigation task, showing that our models can learn a cognitive map of the underlying space and generalize OOD (e.g., to longer sequences) with near-perfect performance, unlike current architectures. Together, these results demonstrate the superiority of models designed to learn a cognitive map, and the importance of introducing a structural bias for structure-content disentanglement, which can be achieved in Transformers with input-dependent positional encoding. *MapFormers* have broad applications in both neuroscience and AI, by explaining the neural mechanisms giving rise to cognitive maps, while allowing these relation models to be learned at scale.

1 Introduction

The ability of Transformers [3] to process sequences in parallel has enabled the training of Large Language Models (LLMs) on increasingly large datasets, creating models able to write poetry, solve complex mathematical problems, or even describe what they observe in an image, results so impressive that debates about their reaching AGI (Artificial General Intelligence) have already started [4, 5]. Yet, the same models learn incoherent world models [6], make logical mistakes on tasks that are trivial to us humans [7], and even when they are right, they can be so for the wrong reasons [8]. Moreover, the fact that different architectures lie at different levels within Chomsky’s hierarchy of language [9] suggests that a key structural bias is still missing in order to reach human-like generalization abilities and AGI.

In comparison, human and animal cognitive abilities appear much more robust and flexible. It has been suggested that the reason for this is our ability to build *cognitive maps* [10], internal models of the relationships among entities or events in the world (Figure 1a). This definition was first introduced in 1948 by Edward Tolman [11] as a way to explain how rats could successfully find new routes

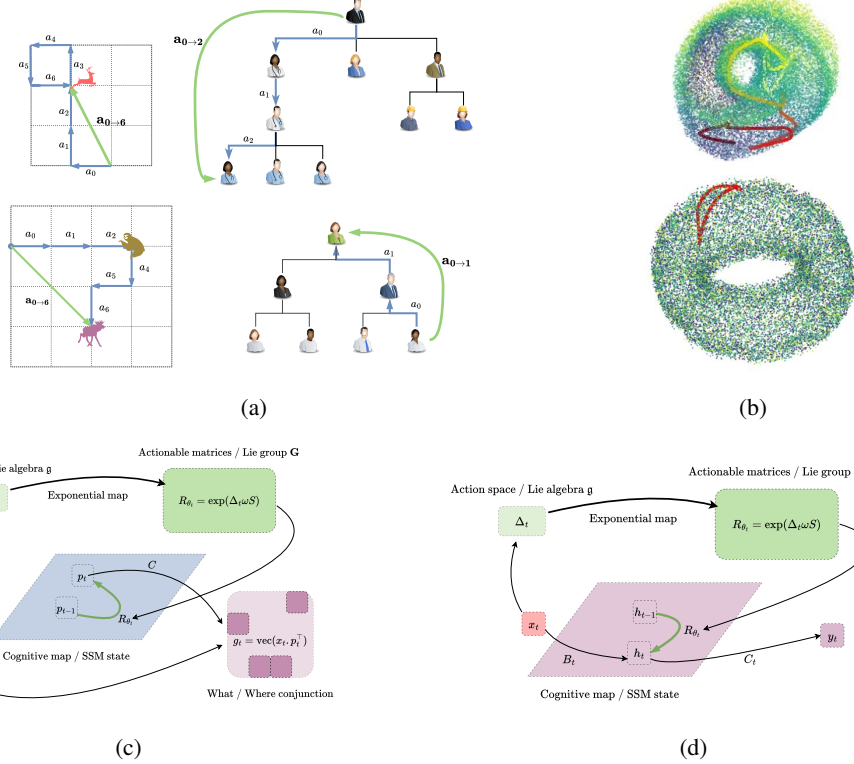


Figure 1: Cognitive Maps: Disentangling Structure and Content for Path Integration in Episodic and Working-Memory Models. (a) Cognitive maps model the relationships between entities, such as objects in space or people working in an organization. In a cognitive map, both the entities and their position are represented but they can be *factorized* from each other. The position (or, more generally, the ‘state’) in a cognitive map is updated via *actions* (blue arrows). For example, actions can update position on a grid (e.g., ‘step right’ in the left drawings), or in more abstract environments, on an organization chart (e.g. ‘the boss of’, on the right). Actions are assumed to have the same effect on the state in the map across all positions and across all environments (up vs bottom). *Path integration* can be achieved by sequentially combining actions together $a_{0 \rightarrow T} = (a_0 \rightarrow \dots \rightarrow a_T)$ (green arrow). (b) (Top) The mental trajectory of a rodent navigating a maze lies on a torus (figure adapted from [1] under CC BY 4.0 license); (bottom) trajectories during a 2D navigation task in *MapFormers* also lie on a torus. The red curve represents a square trajectory performed by the simulated agent during a navigation task, returning to its initial starting point, as desired. (c-d) An illustration of the conceptual framework behind *MapFormers*, and of the differences between the two variants for Episodic Memory (EM) and Working Memory (WM) models [2]. (c) **Episodic Memory (EM) model:** Positions (or ‘states’, more generally) in a cognitive map p_t ’s (in blue), at times t ’s, are encoded in a separate neural space by, e.g., a dedicated neural population. Such population does not directly interact with the input x_t (red), but its state is updated via actions only. Actions a_t ’s, when they occur in the input, can update the position via input-dependent matrices W_{a_t} (green): $p_t = W_{a_t} p_{t-1}$. W_a ’s are input-dependent matrices and are computed through an exponential map, which maps between abstract representations of actions A ’s (residing in the Lie-Algebra space) and the corresponding weight matrix W_a ’s (in the corresponding Lie group; section 3.4). The exponential mapping is computed based on the integration time Δ_t of the action (light green) – roughly, for how long the action needs to be applied. Finally, the conjunction (purple) of the content (the ‘what’) and the structure (the ‘where’) can be computed. (d) **Working Memory (WM) model:** In contrast to the EM model, which factorizes content (red) and position (blue) in two separate neural spaces, *MapFormers*-WM represent position implicitly. Actions in the WM model directly update the conjunction of what and where (purple). The conjunction states h_t ’s in the WM model are thus smaller by a quadratic factor compared to the EM model.

in a maze after old ones were blocked, behavior that cannot be explained by simple conditioning,

suggesting that rats develop an internal cognitive map of their environment to flexibly adapt to new scenarios. Neural evidence of internal maps was first discovered in the hippocampus [12], with *place cells* firing every time a rodent came back to a specific location. Later, *grid cells* were found in the entorhinal cortex (EC) [13], firing periodically with a “grid-like” pattern as an animal was exploring a room, adding further evidence of an internal map within mammal’s brains.

Cognitive maps are essential for generalization and flexible decision-making, as they provide an internal model that represents the structural relationships among entities in the world. This abstraction holds true for both spatial navigation (e.g., finding a shortcut to get back home, or finding a detour around an obstacle) and non-spatial, conceptual information (e.g., inferring family relations). For example, in the case of spatial navigation, if a wall blocks the road ahead, understanding that the sequences $(\rightarrow, \rightarrow)$ and $(\uparrow, \rightarrow, \rightarrow, \downarrow)$ are equivalent allows an agent to ignore unexpected obstacles by simply walking around before continuing on the desired path. If someone says “Bob is the brother of Alice’s mother,” when asked “Who is Alice’s uncle?” one can easily reply “Bob” by simply knowing the abstract relationships of a family tree. Seeing structure as a connected graph of relations unifies spatial and non-spatial cognitive maps, and is the reason why some have theorized that the neural mechanism allowing the creation of spatial cognitive maps might be “recycled” in humans to build abstract knowledge graphs [14, 15, 16] (fig. 1a).

Cognitive maps achieve robust generalization by separating the abstract, invariant structure of the world from the transient, variable content of observations. Because cognitive maps define the position of an object via its relations to other entities in the world, these models can be formalized as graphs, whose nodes represent objects and edges the relations connecting them [17]. This factorizes **what** has been identified from **where** it was seen. Making structure independent from content dramatically helps generalization, assuming that the structural relations learned in one environment remain true in new ones. Indeed, making a step right then left brings us to the same point whether we perform it in Paris or New-York, while our representation of numbers remains the same whether we are counting apples or oranges. Disentangling structure from content also decreases the required amount of training data by a quadratic factor, since the joint distribution can be expressed as the product of its two marginals: $P(x_i, p_j) = P_x(x_i)P_p(p_j)$. In a world where structure remains stable but observations are infinite, this factorization is fundamental.

In addition to learning the structural relations among entities, an agent must also learn the set of *actions* that affect its state within that structure and how these actions combine. Learning the effect of actions on the state is important for efficient encoding of the underlying structure. For example, knowing how the four cardinal directions (North, South, East, West) combine is enough to define any new trajectory on a grid, while the group of integers $(\mathbb{Z}, +)$ needs only 0, Peano’s successor operation $+$ and its inverse $-$ to infer an infinity of numbers. Once structural relations and actions are represented, an agent can use them to mentally keep track of its position (or more generally, the state) and to simulate the impact of future trajectories [18], a process known as *path integration* (fig. 1a). Humans and animals are highly proficient at path integration [13, 19, 20], which provides two key advantages. First, it allows the agent to maintain an accurate internal estimate of its location even without external sensory input. Second, this ability to mentally integrate actions along the structure allows for the representation of planned actions, which is essential for flexible decision-making and rapid adaptation to unexpected obstacles.

What kind of structural bias must be introduced into a deep learning architecture to enable it to effectively learn a cognitive map and perform robust path integration? Previous work made progress in modeling cognitive maps with RNNs with action-dependent matrices [17], allowing them to solve structure-dependent tasks and perfectly generalize to unseen scenarios. This work also explains the duality between episodic and working memory (EM / WM) [2]: EM uses action-dependent matrices to sequentially update a separate pool of neurons representing the agent’s abstract location in a cognitive map, used for long term recall of structured memories stored in synaptic weights (fig.1c); WM uses these matrices to directly move the state into distinct neural subspaces — acting as memory slots — allowing the model to keep the whole structure in neural activity (fig.1d). Although very promising, these models do not scale since (1) their action-dependent matrices need to be sequentially multiplied to perform path integration, making them slow to train and incompatible with parallel sequence processing, and (2) the models can only be applied to problems where the underlying structure is already known (for example, where the number of actions is known rather than learned).

To address this, we introduce *MapFormers*, a class of transformers that learn context-dependent cognitive maps with a generic neural mechanism, allowing the learning of structure at larger scale. *MapFormers* compute path integration *in parallel* and therefore allows scaling up to complex problems. Furthermore, *MapFormers* are trained in a fully self-supervised manner, and learn by themselves to disambiguate between two types of tokens (actions and observations), which have opposite effects on the learned representations. The former update the internal state’s structure via learned operations but leave its semantic content untouched while the latter leave the internal structure fixed but change the state’s content. Empirically, we argue that *MapFormers*, to the best of our knowledge, are the first generic architectures to learn cognitive maps and generalize to longer sequences without supervision, and with minimal assumptions about the underlying structure. We introduce two variants of *MapFormers*, which unify relative rotary (RoPE [21]) and absolute positional embeddings, respectively as models of working and episodic memory. We confirm the fundamental role that action-dependent positional embeddings play in encoding the location of tokens within a context-dependent cognitive map [22]. Finally, we draw theoretical arguments from Lie-group theory to characterize the class of structures that sequence-processing models are able to learn, allowing us to show that diagonal matrices used in current selective State Space Models are not expressive enough to learn cognitive maps.

2 Related Literature

In seminal work [17], the authors presented a set of tasks, for both spatial (navigation) and non-spatial (e.g., family trees) problems, which require learning a cognitive map in order to achieve strong generalization abilities. The Tolman-Eichenbaum Machine (TEM) was suggested as a model that can learn cognitive maps to solve these tasks. Specifically, TEM is an RNN-based architecture that sequentially updates its internal position with action-dependent weights, before querying a Hopfield memory module [23] with its updated position to retrieve what has been seen at a previously visited location.

To extract and build a cognitive map from observational input and, in particular, to learn how an action taken affects the current position in the map, TEM suggests moving beyond standard RNNs. In standard RNNs, the recurrent weight matrix is fixed and applied to any input in the same way. However, rules need to be dynamically applied or not depending on context. In order to model how input actions update the current position in a cognitive model, the weight matrix must depend on the input. That is, instead of having a fixed weight matrix W , the model needs to learn an *input dependent* matrix, specific to each action.

The TEM framework was originally suggested as a computational model of the entorhinal and hippocampus regions in the Medial Temporal Lobe (MTL) for the encoding of cognitive maps in long-term episodic memory (EM), explaining the role of the hippocampus in spatial and non-spatial generalizations. In a subsequent extension of this work, [2] broadened the framework to explain how cognitive maps can also be acquired by a different system, proposing a model of the role of the prefrontal cortex (PFC) for working memory (WM) for sequence memory tasks. The WM-based model achieves this without an explicit separation of the content from the learned map structure, instead employing dynamic encoding mechanisms to update structured activity slots.

However, a key limitation of models based on standard RNNs — including both the EM and WM architectures — for large-scale applications is the inherent computational bottleneck created by their sequential processing. This is particularly restrictive in real-world scenarios, such as long-range path integration, where the cumulative effect of a sequence of actions requires the slow, iterative multiplication of recurrent weight matrices. It is best illustrated in TEM-t [22], where it is shown that TEM can be seen as a Transformer, which however loses its parallel sequence processing abilities due to the sequential update of positional embeddings.

To keep path integration compatible with the parallel processing ability of Transformers, we take inspiration from the *input dependent* matrices of modern selective State Space Models [24] and their established links with Transformers [25] to enable path integration in parallel and update all positional embeddings at once. We also introduce theoretical arguments from Lie-group theory to characterize the class structure that a model can learn based on the characteristics of its recurrent matrix, showing that the diagonal matrices used in Mamba models — necessary to scale these architectures — are not expressive enough to learn cognitive maps. From this, we propose two new architectures based on

the Transformer framework for learning both EM-based and WM-based cognitive maps in a fully self-supervised setting (fig. 1c and 1d, fig. 2).

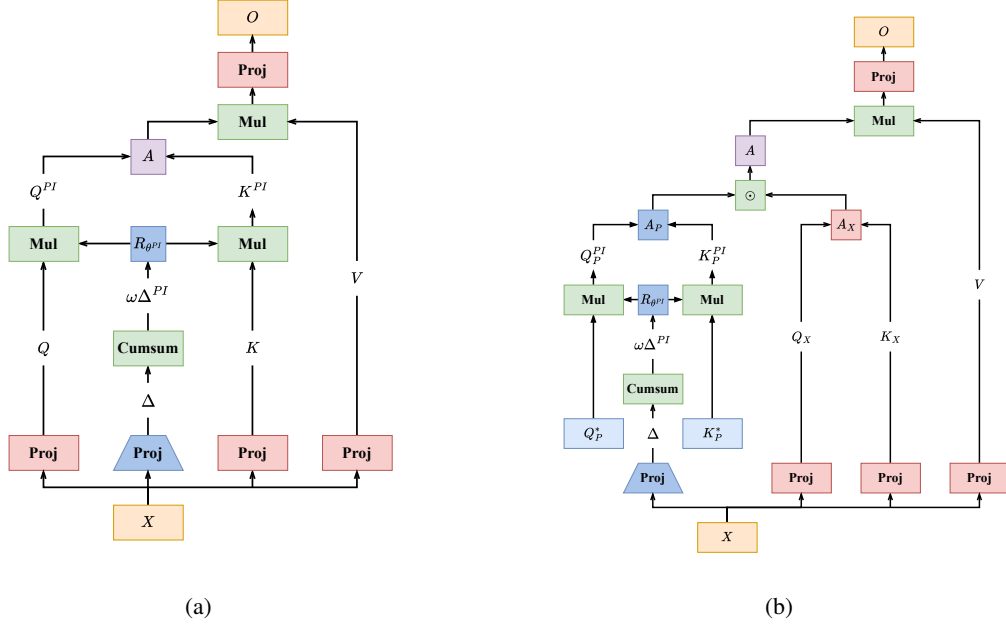


Figure 2: **MapFormers: Path-Integration Transformer-Based Models that Learn Cognitive Maps.** Overview of our Transformer architectures unifying working and episodic memory as relative and absolute positional encodings, respectively. In both cases, rotation angle θ is obtained via a low-rank projection of input X , before applying a cumulative sum (cumsum) along the temporal dimension, to perform **path integration** (PI) in parallel $\theta^{PI} = \omega\Delta^{PI} = \omega \sum_{s \leq T} \Delta_s$. **Input-dependent** block-diagonal matrices computed via $R_{\theta^{PI}} = \exp(\theta^{PI} S)$, $S := -S^\top$ capture the task’s latent structure, while diagonal matrices used in selective SSMs do not. (a) Working Memory *MapFormer (MapWM)* with relative positional encoding, where Q, K are rotated via input-dependent matrix $R_{\theta^{PI}}$. In *MapFormers*, θ is learned, but keeping it fixed gives exactly RoPE (b) Episodic Memory *MapFormer (MapEM)* with two parallel attentions A_X and A_P . The former captures raw similarities between external inputs and the latter encodes the problem’s structure. Combining these two attention matrices with element-wise multiplication $A := A_X \odot A_P$ is equivalent to computing a single attention A_G where keys and queries are the conjunction of observation and position: $g_t = \text{vec}(x_t^\top \cdot p_t) \in \mathbb{R}^{d^2}$, like in TEM-t [22]. In *MapEM*, absolute position embeddings are obtained via path integration of initial and shared key/query positions Q_P^* and K_P^* .

3 General Setup

This section provides the theoretical details that motivate the development of *MapFormers*, as well as their implementation details. Section 3.1 describes the tasks we used for evaluating the models: (1) A selective-copy task and (2) Forced-Navigation tasks. Section 3.3 describes the framework for action-dependent matrices and their formulation as a group. Section 3.4 introduces the idea that for learning a cognitive map, path integration can be more efficiently computed at the Lie algebra vector space, rather than at the group level. Finally, given these insights from Lie theory, 3.5&3.6 show how to build state-space models (SSMs) and Transformer-based models, respectively, that can learn a cognitive map.

3.1 Task

Selective Copy This task was introduced in Mamba [24] to ensure that models are able to ignore distractors, which transformers with static positional encoding like RoPE [21] are unable to do. Intuitively, the model has to “compress” the distances between tokens, and increment its position within the cognitive map (here the number line) every time it sees a non blank token. Solving

this task requires a flexible gating mechanism that baseline transformers do not possess. The model receives a sequence of symbols and must copy it entirely while ignoring a blank token $B : CFEABABBCBF \rightarrow CFEAACF$.

Forced-Navigation Task Following the task proposed by [17], we formulate the learning problem within a standard self-supervised setup. An agent is presented with a set of inputs: s_1, s_2, \dots and its goal is to predict the next input token. We assume that this stream of inputs can contain both sensory observations (e.g., a dog) and actions (e.g., move left). To efficiently solve the task, and generalize OOD, the model needs to learn the hidden structure in the input (e.g., the position of the dog and the relationship of this position to other positions of other input tokens) and separate it from its contingent content (i.e., the dog itself in this position, which might be another animal in another environment). In other words, the model needs to learn to build a cognitive map. Learning this cognitive map also means to identify which input tokens s_t correspond to actions, as well as learning how these actions affect the current, ‘active’, position in the cognitive map.

It is important to note here that even though the model receives a sequence of symbols and effectively does not purposely take any action, it must nonetheless infer the meaning of each symbol without any supervision. Indeed, it sometimes happen to simply follow a schematic sequence of instructions (ex: “Turn right then left at the end of the tunnel”) and infer one’s position accordingly.

3.2 Baseline models

In all our experiments, we will compare our models to RoPE [21] and CoPE [26]. RoPE is used as our baseline Transformer since it is the most popular (fixed) position encoding architecture, therefore incapable of learning input-dependent matrices, and as we will see, structure-based problems. CoPE is an enhanced Transformer architecture that learns a gating mechanism akin to Mamba SSMs, allowing them to adapt their position encoding by compressing relative distances between tokens, and solve structure dependent tasks such as selective copy. CoPE will serve as a baseline for structure learning models.

3.3 Action-Dependent Matrices Form a Lie Group

As discussed above, the key idea to learn a cognitive map is to move beyond fixed matrices and learn action-dependent matrices, specific to each input action. In [27], the authors introduce *actionable representations* using group and representation theory, as a formalism to map an input action $a \in \mathbb{R}^r$ (e.g. in 2D, $r = 2$ and ‘move right’) to a neural transformation $W_a \in M_n(\mathbb{R})$ (e.g., the corresponding weight matrix of a neural network that implements the effect of this action on the represented position in space p):

$$\begin{aligned} \phi : \mathbb{R}^r &\rightarrow M_n(\mathbb{R}) \\ a &\mapsto W_a \end{aligned} \tag{1}$$

where ϕ_a acts on the representation $p \in \mathbb{R}^n$ (e.g., abstract position in space) such that $p(x + a) = W_a p(x)$. We refer to the matrices W_a ’s as action-dependent matrices, since unlike standard RNNs, the weight matrix may depend on the specific action taken. To be useful for updating positions in cognitive maps, the action-dependent matrices need to form a group, and specifically, in addition to (1) closure and (2) associativity, it needs to satisfy the following properties: (3) include a matrix for the null action: $W_0 = \mathbf{I}_n$, (4) $\forall a : W_a$ is invertible with inverse W_{-a} (e.g., ‘one step right’ has the exact opposite effect on the neural representation of ‘one step left’ - $\forall x, a : p(x + a - a) = W_{-a} W_a p(x) = p(x)$). In summary, the requirements for a neural representation for a cognitive map to be consistently and reversibly updated by actions (including a null action and an inverse for every action) mean that the set of action matrices $\{W_a\}$ must constitute a subgroup of the General Linear Group, $GL(n, \mathbb{R})$, under matrix multiplication. Note that this results in various desired properties, such as making the actions a ’s invariant with respect to the specific position p they update – In the absence of noise, the action has the same effect on any of the represented positions. Indeed, making the same step right should update the position in the same way whether we are in Paris or New York.

The insight that action-dependent matrices need to form a group, and in particular a Lie group over \mathbb{R} , allows the use of results from group and representation theory to understand what are the possible constraints on the form of W_a ’s [27]. Specifically, the Peter–Weyl theorem [28] states that any compact group G can be represented in $M_n(\mathbb{R})$ as:

$$W_a = M \begin{bmatrix} I_1(a) & 0 & \cdots & 0 \\ 0 & I_2(a) & \cdots & 0 \\ \vdots & \vdots & \ddots & \vdots \\ 0 & 0 & \cdots & I_d(a) \end{bmatrix} M^{-1} \quad (2)$$

where I_k are called the *irreducible representations (irreps)* of group \mathbf{G} and M is an invertible matrix. This representation of action-dependent matrices, through the irreps of the group \mathbf{G} , provides insights into which core actions can be performed by W_a 's. For example, for navigation on a circle (1D) or torus (2D), the *irreps* are rotations R_{θ_k} :

$$I_k(a) := R_{\theta_k} = \begin{bmatrix} \cos(\omega_k \cdot \Delta_{t_k}) & -\sin(\omega_k \cdot \Delta_{t_k}) \\ \sin(\omega_k \cdot \Delta_{t_k}) & \cos(\omega_k \cdot \Delta_{t_k}) \end{bmatrix}; \quad \theta_k = \omega_k \cdot \Delta_{t_k} \in \mathbb{R}, \quad (3)$$

where $\omega_k, \Delta_{t_k} \in \mathbb{R}^r, r = 1, 2$ are the rotation durations and frequencies, respectively, the latter representing movement at different scales. That is, in this example, each I_k performs a rotation of a subspace of the neural space. The matrix M then performs a change of basis on this result, assuming M is not the identity.

3.4 Path Integration Can Be More Easily Computed in the Lie-Algebra Space

To learn a cognitive map, we saw that it is desirable to require action-dependent matrices to form a Lie group \mathbf{G} . A Lie group is a group G that is also a smooth manifold, such that the group operations (multiplication and inversion) are smooth maps. For example, the group of 2D rotations $\mathbf{SO}(2)$ is a Lie group. To build a neural model that can learn cognitive maps, the goal would be to learn action-dependent matrices that form a Lie group.

To further characterize the group of action-dependent matrices, it is often simpler to analyze the corresponding Lie algebra. The associated Lie algebra \mathfrak{g} of a Lie group \mathbf{G} is the tangent vector space of \mathbf{G} at the identity element. Lie-group theory shows the existence of an exponential map between the Lie algebra and the group $\exp(\cdot) : \mathfrak{g} \rightarrow \mathbf{G}$, and in the case of a compact group, where the exponential map is surjective, any element $W_a \in \mathbf{G}$ of the group can be expressed as the exponential of an algebra element A , $W_a = \exp(A) \in \mathbf{G}$. This is useful since studying the structure of Lie groups (which involves, e.g., matrix multiplication) is often simpler from the point of view of the corresponding Lie algebra (which is linear and involves addition operations).

For the case of cognitive maps, we will think of elements of the Lie algebra A 's as action representations, and the corresponding group elements (expressed via the exponential map) as the action-dependent matrices W_a 's, which implement these actions in synaptic weights. The exponential map provides the link between the vector space of actions (the Lie algebra) and the space of weight matrices (the Lie group). Specifically, given the property of the exponential map (if the A_i 's commute): $\exp(\sum_i A_i) = \prod_i \exp(A_i)$, the exponential mapping translates the additive structure of the Lie algebra (cumulation of actions in this vector space - e.g., 'move right' then 'move up') into the multiplicative structure of the Lie group (multiplication of the corresponding action-dependent weight matrices). This is useful for path integration, since the cumulative effect of taking actions A_1, \dots, A_n can be translated to the final action-dependent weight matrix $W_a = \prod_{i=1}^n \exp(A_i)$. As we will see, the exponential map allows in some cases to compute path integration in parallel, in the vector space of the Lie algebra, by first computing the cumulative summation of subsequent actions and only then computing the exponent of the result.

For example, for spatial problems, such as navigation on a circle or a torus, the Lie group of interest is $\mathbf{SO}(2)$ - the group of all 2D-rotations.

$$R_\theta := \begin{bmatrix} \cos(\theta) & -\sin(\theta) \\ \sin(\theta) & \cos(\theta) \end{bmatrix} \quad (4)$$

The corresponding Lie algebra of $\mathbf{SO}(2)$, denoted $\mathfrak{so}(2)$, consists of all 2×2 real matrices A that are skew-symmetric ($A^\top = -A$). The Lie algebra $\mathfrak{so}(2)$ is a one-dimensional vector space, spanned by a single basis *skew-symmetric* matrix $S := -S^\top$ (2D-rotations have a single degree of freedom). Thus, all elements of the Lie algebra can be expressed by a single scalar (the angular velocity) ω as

$A = \omega S$. A finite rotation R_θ can then be seen as generated by integrating the infinitesimal angular velocities ω over a duration Δ_t :

$$S = -S^\top = \begin{bmatrix} 0 & -1 \\ 1 & 0 \end{bmatrix}; R_\theta = \exp(\Delta_t A) = \exp((\omega \Delta_t) S) = \begin{bmatrix} \cos(\omega \Delta_t) & -\sin(\omega \Delta_t) \\ \sin(\omega \Delta_t) & \cos(\omega \Delta_t) \end{bmatrix} \quad (5)$$

Intuitively, the skew-symmetric matrix $A = \omega S$ defines the instantaneous action direction S and constant angular velocity ω . The finite rotation $R_\theta \in \mathbf{SO}(2)$ is obtained by the exponential map, which performs a continuous integration of this velocity. Thus, the expression $R_\theta = \exp(\Delta_t A)$ shows that the final rotation yields a total angle of $\theta = \omega \Delta_t$, which defines the smooth path (geodesic) on the group manifold.

This framework has important implications for learning a cognitive map. Given that all elements of a compact and connected Lie group (the action-dependent matrices in our case, like rotation groups) can be expressed by the exponential of a single linear combination of the associated Lie algebra generators, learning a cognitive map can be simplified: learning can be performed *at the level of the algebra* rather than the non-linear group level. The algebra primarily involves linear operations and summation – which are naturally compatible with modern deep learning frameworks and backpropagation – while the Lie group involves matrix multiplication. This linearization is useful because the linear path integration required by the exponential map can be much more easily parallelized, as we will see further below.

More generally, given the group of action-dependent matrices W_a 's (which, as we saw, needs to be a subgroup of the general linear group $GL(n, \mathbb{R})$), elements of the algebra, $A(t)$, can be expressed by a linear combination of generators A_i 's scaled by parameters t_i 's (the ‘integration times’, which can be seen as coordinates along the different directions defined by the generators). If surjective, all group elements W_a 's can then be expressed using the exponential map (fig.1):

$$\begin{aligned} A(t) &= \sum_{i=1}^D t_i A_i \in \mathfrak{g}, \quad t_i \in \mathbb{R} \quad (\text{Linear combination in the Algebra}) \\ W_a &= \exp \left(\sum_{i=1}^D t_i A_i \right) \in G \quad (\text{Mapped to the Group via Exponential}) \end{aligned} \quad (6)$$

For the special case where the generators A_i commute (i.e., the Lie bracket is zero), as in the simple $\mathbf{SO}(2)$ example, the exponential of the sum equals the product of the exponentials: $W_a = \prod_{i=1}^K \exp(t_i A_i)$. This shows again the benefit of the Lie algebra: it transforms the non-linear composition (multiplication) of the group into linear path integration (addition) within the algebra, thereby facilitating efficient learning and parallelization in the model.

3.5 **MAMPa**: Learning Cognitive Maps with block-diagonal Mamba Models

In this section, we propose a Lie-theoretic interpretation of State-Space Models (SSMs), which provides an interpretation of modern SSMs as models that implicitly perform path integration and can thus learn cognitive maps under certain conditions. This framework reveals a substantial limitation of current state-of-the-art SSMs, such as Mamba and Mamba2 [24, 25], to meet these conditions for learning cognitive maps. We thus propose a simple modification of the Mamba architecture, which we call **MAMPa**, for learning cognitive **Maps** with **Mamba** models.

Recently, structured state-space models (S4) [29] have gained popularity over Transformers as they allow parallelized training of sequences while keeping a linear inference cost. These models are inspired by continuous state space models, where a continuous signal $x(t) \in \mathbb{R}$ is mapped to $y(t) \in \mathbb{R}$ via a hidden variable $h \in \mathbb{R}^n$:

$$\begin{aligned} h'(t) &= Ah(t) + Bx(t) \\ y(t) &= Ch(t) \end{aligned} \quad (7)$$

These continuous systems can be applied to a sequence of discrete tokens, using the zero-order hold (ZOH) rule, which assumes that the input signal $x(t)$ is constant during a step size Δ . This yields the corresponding discrete version of the dynamics:

$$\begin{aligned} h_{t+1} &= \bar{A}h_t + \bar{B}x_{t+1} \\ y_{t+1} &= Ch_{t+1} \end{aligned} \tag{8}$$

where $\bar{A} = \exp(\Delta \cdot A)$ and $\bar{B} = (\Delta \cdot A)^{-1} (\exp(\Delta \cdot A) - I) \Delta B$. This discretization step is fundamental, as it explains how an exponential map can arise from the integration of infinitesimal recurrent transformations over a time interval $\Delta \in \mathbb{R}$.

In Mamba, an improved version of (S4), input selectivity is ensured via a per-token learnable step Δ_t and matrix A , that when combined defines a per-token transformation:

$$\bar{A}_t := \exp(\Delta_t A) \tag{9}$$

The exponential relationship between A (the continuous domain matrix) and \bar{A} (the discrete domain matrix) directly parallels the relationship between the element A of the Lie algebra and the weight matrix W_a in the corresponding Lie group. In the rotation example, since the Lie-algebra $\mathfrak{so}(2)$ of *skew-symmetric* matrices gives rise to the Lie-group of rotation matrices $\mathbf{SO}(2)$, $A := \omega S$ is the infinitesimal generator and W_a is the finite rotation over duration Δ_t : $W_a = \exp(\Delta_t A)$. By identifying the discrete-time SSM matrix \bar{A} with the action-dependent matrix W_a , we propose a new theoretical framework to analyze the capacity of Mamba to learn action-dependent matrices and cognitive maps. In this framework, Mamba can be interpreted as learning action-dependent matrices \bar{A}_t , which are dynamically created via an exponential map. As we saw, the exponential map integrates infinitesimal steps via A (the direction and velocity in the Lie algebra space) over a varying time interval Δ_t , giving a finite transformation \bar{A} (the element of the Lie group). In other words, Mamba implicitly computes *path integration* of action A over a duration defined by the learned parameter Δ_t .

Given this theoretical framework, it is evident that current versions of Mamba are incapable of learning cognitive maps that require, for example, learning rotations. In Mamba, A was chosen as diagonal, to reduce computational cost, but a diagonal action-dependent matrix cannot learn rotations. This is since \bar{A} needs to be similar to a block-diagonal matrix, with blocks of size 2 (eq. 2 & 3). Mamba was shown to be able to learn gating problems, which increases the performance of Mamba on various structure-dependent tasks by ignoring irrelevant information, however, Mamba with a diagonal constraint is not expressive enough to represent spatial cognitive maps as Lie-group theory shows. In this work, we modify A in Mamba to be block-diagonal and, in particular, to blocks of size 2 (for learning rotations) and show that this modification increases the capacity of the model to learn cognitive maps.

3.5.1 MAmPa as a Model of Episodic Memory (EM) and Working Memory (WM)

In [2], the authors introduce two related models of episodic (EM) and working memory (WM) that both learn cognitive maps using RNNs with *input-dependent* matrices. Discrete SSMs can be regarded as RNNs with no activation function, and since selective SSMs learn *input-dependent* matrices, EM and WM models can naturally be regarded as selective SSMs. The EM-RNN model behaves exactly like TEM [17], factorizing structure and content in two distinct neural populations, but only updates its position with an input-dependent RNN $p_t := W_{a_t} p_{t-1}$. It then queries a Hopfield memory module [23] with its updated position to retrieve passed observations. The RNN in TEM can be seen as an SSM with two subtle differences: (1) it uses no external input, *i.e.* $\forall t, x_t = 0$; (2) a learnable embedding p_* representing the cognitive map's *zero coordinate* must be introduced to avoid the state being always null:

$$\begin{aligned} p_t &= \exp(\Delta_t A) p_{t-1} = \exp\left(\omega S \sum_0^t \Delta_s\right) p_* \\ q_t &= C p_t = C R_{\theta_0 \rightarrow t} p_* \\ g_t &= \text{vec}(x_t^\top \cdot q_t) \end{aligned} \tag{10}$$

where C is an optional learnable parameter to project the updated position out of the cognitive map like in standard SSMs, but setting $C := \mathbf{1}_n$ implies that $q_t = p_t$, which is analogous to TEM/EM RNNs (fig. 1c). Moreover, compared to RNN based models, this formulation allows to compute path integration directly in the Lie algebra ($A \sum_0^t \Delta_s$) and avoid sequential matrix multiplication.

WM-RNNs directly updates the internal state with input-dependent matrices, which is exactly what selective SSMs do. As such, current selective SSMs with the appropriate matrix structure (*skew-symmetric* in the case of navigation, eq. 3) naturally model working memory (fig. 1d). This allows us to unify SSMs with EM and WM models, where **the SSM’s inner state-space can now be understood as a cognitive map**.

In the previous section, analyzing SSMs through Lie-group theory has allowed us to understand their current limitations, and that one only needs to switch to block-diagonal matrices to theoretically be able to learn a cognitive map. However, people decided to keep diagonal matrices because it dramatically reduces the computational load. By treating A as a vector, one can avoid computing a matrix exponential and also dramatically reduce the memory footprint of a parallel scan, by computing vector-vector multiplications instead of matrix-vector’s. Even then, Mamba uses a very small inner state $N \approx 16$, showing how difficult it is to scale these architectures. In Mamba2 [25], the authors decide to reduce $A := a \in \mathbb{R}$ in order to scale the inner state’s size $N = 64$ to modern Transformer standards. This highlights a fatal limitations of parallel-selective SSMs: they can be parallelized at the cost of loosing any hope of learning a cognitive map (see sec. 10.1 for further details). This is the reason why we decided to move away from SSMs and adapt Transformers to learn cognitive maps, as models of episodic (*MapFormer-EM*) and working memory (*MapFormer-WM*).

3.6 *MapFormers*: Path-Integrating Transformers for learning Cognitive Maps

In this section, we introduce two new Transformer-based architectures, which we call *MapFormers*, designed to learn path integration and, consequently, cognitive maps. Like RNNs and SSMs, the two proposed architectures primarily differ in how structural and content information are encoded (fig. 1c&d, fig. 2). The first architecture extracts and represents structural information *separately* from the content, using absolute positional embeddings to form a cognitive map; this is akin to a model of episodic memory [17]. The second architecture, conversely, represents the sequential information of both structure and content jointly through relative positional encoding. This can be seen as a model of working memory that utilizes different neural-activity subspaces to store information in distinct memory slots [2]. Crucially, the fundamental mechanism in both *MapFormers* is the use of *input-dependent matrices* to update positional encoding.

As we saw, a key aspect of cognitive maps that explains their contribution to OOD generalization is the factorization of content and structure in the input. In Transformers, this factorization can naturally arise when using input-dependent positional embeddings. To see this, we will start by reviewing the Transformer architecture.

The attention mechanism in Transformers is what has allowed the parallel processing of sequences, and therefore the ability to scale training on large scale datasets. An input sequence $X \in \mathbb{R}^{t \times d}$ is projected into keys, queries and values, $Q, K, V \in \mathbb{R}^{t \times d}$, and token mixing is achieved via a weighted sum of the values based on the key-query similarity matrix $A \in \mathbb{R}^{t \times t}$:

$$\text{Att}(Q, K, V) = \text{softmax} \left(\frac{QK^T}{\sqrt{d}} \right) V \quad (11)$$

Since the attention mechanism is agnostic to the position in the sequence (and therefore invariant to permutation of the input), for many tasks, such as language modeling, positional information needs to be provided. There are two general approaches to introduce positional information – absolute positional and relative positional embedding. In the case of absolute positional embeddings, the embeddings of input token x_i ’s is combined with positional information via: $x_i \mapsto x_i \odot p(i)$, where \odot can be any binding operation, usually $+$ or \times . These absolute positional embeddings p_i ’s $\in \mathbb{R}^d$ can be either learnable embeddings or fixed (e.g., vectors of sines and cosines at different frequencies [3]). In the case of relative positional encoding, a function $e(i, j)$ is directly applied to the attention mechanism, to represent the relative position between a query q_i and key k_j : $a_{ij} \mapsto a_{ij} \odot e(i, j)$.

3.6.1 *MapFormers-EM*: *MapFormers* with Absolute Positional Embeddings as Models of Episodic Memory (EM)

We begin by introducing the first architecture of *MapFormers*, which makes use of absolute positional embeddings to learn a cognitive map, inspired by the links established between TEM and transformers (TEM-t [22]). The key idea is to encode positions in a cognitive map using the keys and queries of the positional embeddings p_t ’s, which are separated by design from the token embeddings x_t ’s. For encoding a cognitive map, where the position in the map depends on previous actions in the

input, fixed positional embeddings (e.g., vectors of sines and cosines at different frequencies [3]) would clearly not suffice since they can only represent a fixed structure (linear order), and therefore positional embeddings that are learned from the input are needed, i.e., input-dependent positional embeddings. This generalizes the notion of positional embeddings, which can now be understood as representations of the model’s position in an abstract, context-dependent cognitive map, and not simply position in the sequence.

To see how a cognitive map can be implemented via positional embeddings, we illustrate it with the example of navigation in 1D. We model the 1D movement on a circle rather than a line, since this enforces periodicity and prevents the positional representation from diverging (as opposed to exponential gating used in Mamba who’s inverse diverges towards infinity), allowing the model to naturally handle boundary conditions. The model’s objective is to track the absolute position p_t at step t , which is updated after each action via a rotation matrix R_θ . This position p_t must be the result of path integration: the summation of all preceding actions in the input sequence. The key realization here is that path integration is simpler to compute in the Lie Algebra vector space, rather than in the Lie Group space (where positions are updated by costly matrix multiplication; section 3.4). In the linear Lie Algebra space, path integration is learned by simply adding up the small integration durations Δ_t ’s for each time step. Since this mechanism relies on a parallelizable summation operation, the Transformer architecture is ideally suited for this task, ensuring fast and efficient training and path computation.

In practice, path integration of the various Δ_t ’s across time is performed using a cumulative sum (cumsum) (fig.2b). For example, in the case of 1D navigation, each action token in the sequence is first projected onto a one-dimensional vector (a scalar in this case), which represents the integration time Δ_t . The cumsum operation then computes, for each token, the estimated cumulative integration time $\sum_{i \leq t} \Delta_i$ (the total path length traveled so far). To compute the corresponding cumulative rotation angle (θ_t) for each token, the cumulative integration time needs to be multiplied by the angular velocity ω , a parameter learned by the model. In fact, to encode the full position in the cognitive map, the model learns a set of these frequencies (ω ’s), which jointly estimate the position in the map. These ω ’s are analogous to the different frequencies ($\omega = 2\pi f$) used in standard fixed positional embeddings. Given the cumulative integration time and the learned frequencies, the rotation angle at time t is computed. The next step is the re-entry into the Lie Group space: using the exponential map, we translate the linear path integration result from the Lie Algebra (addition) back into the action-dependent rotation matrices (elements of the Lie Group). This performs the required operation without needing to compute expensive matrix multiplication at every step by exploiting the property of the exponential map: $\exp(\sum_i \Delta_i A) = \prod_i \exp(\Delta_i A)$. In practice, for navigation problems, the matrix exponentiation does not need to be computed because the resulting form of the rotation matrix is already known (eq. 3). The resulting θ_t ’s from the path integration can thus be simply introduced into the rotation matrices, which then multiply the keys and queries of the positional embeddings.

Finally, the keys and queries of the positional embeddings, K_P and $Q_P \in \mathbb{R}^{t \times d}$, are the vectors that encode the position in the cognitive map. Their starting point p_* , encoded by $k_*^p, q_*^p \in \mathbb{R}^d$, represents the zero coordinate of the cognitive map and is learned as another set of parameters by the model. For each token in the sequence, these initial zero-coordinate vectors are updated by multiplying them with the action-dependent matrices W_a ’s (the rotation matrices R_θ ’s in the case of navigation). These matrices represent the cumulative effect of the path integration, computed using the exponential map as described above. That is:

$$p_t := W_t p_{t-1} = \left(\prod_{s=1}^t W_s \right) p_* = \exp \left(\omega S \sum_{s=1}^t \Delta_s \right) p^* = R_{\theta_{0 \rightarrow t}} p_* := \mathbf{PI}_{0 \rightarrow t} \quad (12)$$

As we saw, the path integration thus avoids matrix multiplication and is replaced by the cumsum $\sum_s \Delta_s$, before computing matrix exponential, allowing scaling of this operation to much longer sequences by computing it in parallel. This contrasts with TEM-t, that sequentially updates its positional embeddings, loosing the parallel processing abilities of transformers.

The updated positional embeddings (K_P and Q_P) constitute a ‘neural population’ encoding of the cognitive map. At each time step t , the resulting vectors k_t^p and q_t^p encode the path-integrated position p_t . This positional module operates autonomously, equivalent to an SSM driven solely

by internal dynamics (eq.10). The attention of *MapEM* mimics the role of the Hopfield module in EM-SSMs/RNNs, used to retrieve passed memories with the conjunction of **what** has been seen and **where**: $g_t = \text{vec}(x_t^\top \cdot p_t)$ (fig.2b). We extend this logic, such that the final positional keys and queries $k_i^g = \text{vec}(k_i^{x^\top} \cdot k_i^p)$ and $q_j^g = \text{vec}(q_j^{x^\top} \cdot q_j^p)$ reflect this conjunction.

Since $\forall i, j : \langle g_i, g_j \rangle = \langle q_j^{x^\top} \cdot q_i^p, k_i^{x^\top} \cdot k_j^p \rangle = \langle q_j^x, k_j^x \rangle \langle q_i^p, k_j^p \rangle$, we can avoid the outer products $Q_X^\top Q_P$ and $K_X^\top K_P$ by computing content and position attentions $A_X = \text{Att}(Q_X, K_X)$ and $A_P = \text{Att}(Q_P, K_P)$ separately (still in parallel by concatenating the heads), such that A_P acts as an attention mask on A_X :

$$(\text{Att}(Q, K) \odot \text{Att}(Q_P, K_P)) V = (\mathbf{A}_X \odot \mathbf{A}_P) V \quad (13)$$

3.6.2 *MapFormers* with Relative Positional Embeddings as a Model of Working Memory

As explained before, it was suggested that the brain encodes the structure of sequences, builds cognitive maps and stores them using two different systems: (1) Episodic Memory (EM), which stores a conjunction of structure and content information in long-term memory, as we saw previously, and (2) Working Memory (WM), which encodes sequential information without an explicit separation of the content from the learned map structure. Instead, WM employs dynamic encoding mechanisms to update structured activity slots.

In Transformers, position encoding can be achieved in a separate neural population, which mimics EM models with absolute positional embeddings, or by directly rotating the keys and queries to encode relative distances, like in WM models that directly update the state. The most popular positional encoding method is called RoPE (Rotary Positional Embeddings, [21]), where each key and query is rotated by 2×2 block-diagonal rotation matrices $q_i, k_j \mapsto R(i)q_i, R(j)k_j$ such that the attention mechanism computes:

$$a_{ij} := \text{RoPE}(q_i, k_j) := (R(j)k_j)^T \cdot R(i)q_i = k_j^T R(i-j)q_i \quad (14)$$

Since the transpose of a rotation matrix is also its inverse, the key-query dot product naturally relates to a rotation dependent on the distance $i - j$. This property suggests a potential for implementing path integration (PI) in the form $\bar{q}_j^\top \cdot \bar{k}_i = q_j^\top R_{\theta_{PI_{i \rightarrow j}}} k_i$. However, the rotation matrices in standard RoPE are fixed, depending only on the positional distance $i - j$. To learn the action-dependent matrices required for building a dynamic cognitive map, RoPE needs to be modified. This is achieved in *MapFormers*-WM by learning the rotation angle θ_t (and thus the matrix R_t) from the input context x_t , making it selective. Compared to simple gating, which only maintains or suppresses information, learned rotations allow tokens to interact in similar subspaces or ignore each other by rotating into orthogonal subspaces.

For efficient computation and fast parallelization, both *MapWM* and *MapEM* implement *linear* path integration. This is achieved using cumulative summation (cumsum), as illustrated in fig. 2. During the training process, the model learns both the integration times (Δ_t 's) and the angular velocities (θ_t 's). In contrast to EM, the Working Memory (WM) approach results in the entanglement of structural and content information within the resulting positional embedding keys and queries (K_{PI}, Q_{PI}), reflecting the integrated nature of sequential encoding in WM.

3.7 Relationship between *MapFormers* and *MAMPA*: Linear *MapFormers* are selective SSMs

In the previous section, we have introduced the exponential map in Transformers to allow them to build *input-dependent* matrices and learn cognitive maps. The Transformer formalism cannot naturally explain how an exponential map emerges like in SSMs, but in Mamba2 [25], the authors show that linear transformers [30] are actually SSMs. Starting from equation 8:

$$\begin{aligned} h_t &= A_t h_{t-1} + B_t x_t \\ &= A_t \dots A_1 B_0 x_0 + A_t \dots A_2 B_1 x_1 + \dots + A_t A_{t-1} B_{t-2} x_{t-2} + A_t B_{t-1} x_{t-1} + B_t x_t \\ &= \sum_{s=0}^t A_{s \rightarrow t}^\times B_s x_s; \quad A_{s \rightarrow t}^\times := \prod_{i=s+1}^t A_i \end{aligned} \quad (15)$$

after multiplying by C_t , we get the final equation:

$$\begin{aligned} y_t &= \sum_{s=0}^t C_t^T A_{s \rightarrow t}^\times B_s x_s \\ \Rightarrow y &= Mx; \quad m_{ij} := C_j^T A_j \dots A_{i+1} B_i \end{aligned} \tag{16}$$

If we remove the matrices A_t , the matrix $M := (m_{ij}) : m_{ij} = C_j^T B_i := q_j^T k_i$ can be seen as the key-query similarity matrix QK^T without softmax normalization, as in linear transformers. Equation 16 is fundamental as it characterizes exactly how actionable representations can be implemented in transformers, where matrix $A_{i \rightarrow j}^\times = A_j \dots A_{i+1}$ represents the model's path integration between tokens i and j .

If we choose matrix $A := S$ to be a 2×2 block-diagonal skew-symmetric matrix and $R_t := \exp(\theta_t S) = \exp(\Delta_t \omega S)$ as in equation 5, we retrieve equation 14:

$$\begin{aligned} m_{ij} &= q_j R_{i \rightarrow j}^\times k_i \\ &= q_j^T R_{0 \rightarrow j}^\times (R_{0 \rightarrow i}^\times)^{-1} k_i \\ &= (\bar{R}_j q_j)^T (\bar{R}_i k_i); \quad \bar{R}_i := (R_{0 \rightarrow i}^\times)^{-1} = \exp\left(-\sum_{s=0}^i \Delta_s \omega S\right) := \exp\left(\sum_{s=0}^i \theta_s S\right) \\ &= \text{RoPE}(q_j, k_j) \end{aligned} \tag{17}$$

This proves that linear RoPE transformers are SSMs with a 2×2 skew-symmetric recurrent matrix, where θ_t controls the angle of rotation. In Mamba2, the authors define $A := a \in \mathbb{R}$ as a scalar, giving $M_{ij} = \exp(-a \sum_{t=i+1}^j \Delta_t) q_j^\top k_i$, which is analogous to the cumulative gating of CoPE (Contextualized Positional Encoding) [26], with a multiplicative and not additive binding operation. CoPE is an enhanced Transformer architecture with context-dependent positional encoding, that like Mamba compresses the relative key-query distances with a cumulative gating mechanism, and in both models, input selectivity allows them to focus or ignore certain tokens and solve structure-dependent tasks, but should not allow them to learn spatial cognitive maps.

This ends our unification of *MAmPa* and *MapFormers* with EM and WM RNNs. The formalism of SSMs allows us to understand how *input-dependent* matrices are created while computing *path integration* in parallel. Insights from Mamba2 allow us to unify relative positional embeddings with models of working memory, and complete the understanding of cognitive maps in transformers started in TEM-t [22]. Finally, our analysis of SSMs through Lie-group theory demonstrates that diagonal matrices – necessary to reduce computation and scale SSMs – are not enough to learn spatial cognitive maps, leaving only *MapFormers* as realistic models of cognitive maps at scale.

4 Implementation details

We chose rotation matrices because they are well suited to represent most bounded commutative structures (like movement on a finite grid or integers modulo N), but also because they have useful numerical properties: (1) rotations and their inverse are orthogonal and therefore ensure numerical stability, not present in Mamba, since the inverse of the exponential gating matrix they use diverges towards infinity, making it impossible to represent both an action and its inverse in a numerically stable way; (2) their transpose is also their inverse, implying that the key-query dot product $\bar{q}_j^\top \bar{k}_i = q_j^\top R_{PI_{i \rightarrow j}} k_i$ represents path integration between tokens i and j , necessary to learn cognitive maps in parallel.

Rotations can be ensured by enforcing $S := \bar{S} - \bar{S}^\top$ to be skew-symmetric, but since a single generator matrix S can only generate rotations along a single axis (see sec.10.4.2 for further details), choosing blocks of size $b > 2$ is useless as it increases the computational load while effectively reducing the amount of rotations being performed. Using blocks of size 2 also allows us to use the explicit *irreps* representation of 2×2 rotations and avoid computing a matrix exponential (eq.3). This also allows, as in RoPE [21], to rewrite matrix multiplication of $R_\theta x$ in *MapFormers* as:

$$R_\theta x = \begin{pmatrix} x_1 \\ x_2 \\ \vdots \\ x_{d_h-1} \\ x_{d_h} \end{pmatrix} \odot \begin{pmatrix} \cos(\Delta_{t_1} \cdot \omega_1) \\ \cos(\Delta_{t_1} \cdot \omega_1) \\ \vdots \\ \cos(\Delta_{t_{n_b}} \cdot \omega_{n_b}) \\ \cos(\Delta_{t_{n_b}} \cdot \omega_{n_b}) \end{pmatrix} + \begin{pmatrix} -x_1 \\ x_2 \\ \vdots \\ -x_{d_h-1} \\ +x_{d_h} \end{pmatrix} \odot \begin{pmatrix} \sin(\Delta_{t_1} \cdot \omega_1) \\ \sin(\Delta_{t_1} \cdot \omega_1) \\ \vdots \\ \sin(\Delta_{t_{n_b}} \cdot \omega_{n_b}) \\ \sin(\Delta_{t_{n_b}} \cdot \omega_{n_b}) \end{pmatrix} \quad (18)$$

leaving only frequencies $\omega \in \mathbb{R}^{n_b}$ (see sec. 10.2 for a discussion about their initialization) as learnable parameters instead of matrix $S \in \mathbb{R}^{n_b \times b \times b}$.

The actual rotation angle $\theta = \omega \Delta_t$ is dynamically computed from the input features X using a low-rank projection $W_\Delta = W_\Delta^{out} W_\Delta^{in}$. The goal of this two-step process is to ensure the rotation relies only on the most salient action features of the input. First, the internal projection $W_\Delta^{in} \in \mathbb{R}^{d \times r}$ ($r \ll d$) maps the high-dimensional input X to a low-dimensional $\Delta_t^{in} \in \mathbb{R}^{t \times r}$ (for instance, in a 2D environment, Δ_t^{in} could be the 2D movement vector $\Delta_{t_k} \in \mathbb{R}^r$ in eq. 3, where $r = 2$). Second, this extracted action is projected by W_Δ^{out} into the final set of path increments $\Delta_t \in \mathbb{R}^{t \times n_h \times n_b}$, which controls the rotation angle for all attention heads (n_h) and all diagonal blocks (n_b), where $n_b = d_h/b$ is the number of blocks per head dimension.

Finally, compared to TEM and TEM-t that use a single neural population p_t to encode position, our *MapFormers* use two separate initial vectors k_*^p and q_*^p . This distinction is optional and mimics the formalism of EM-SSMs defined in eq. 10, meaning that we could set $k_*^p = q_*^p = p_*$ without loss of generality. However, we suspect this separation to be beneficial because it would create sparser attention values. Indeed, our positions p_t vary smoothly through path-integration, implying that nearby positions would not be strongly separated, but introducing distinct neural populations for keys and queries could allow the model to find the optimal balance between separation/matching of distinct/similar positions.

The fact that *MapFormer-EM* models rely on observations (content) or structure (position) attention A_X and A_P , allows to balance between the two attention maps to compute similarities. To test the impact of each modality, we introduce three types of EM models: (1) *MapEM-os* relying on both observation and structure to compute attention; (2) *MapEM-s* relying on structure alone and (3) *MapEM-o* relying solely on observation, equivalent to a Transformer without positional embeddings, serving as a control. Note that ideally, the model should learn to balance between observation or structure depending on context, but we decided to leave it for future work. This forced separation is primarily used to highlight the benefits of focusing on different modalities depending on the task.

5 Experiments

We defined different tasks that must all be solved without any supervision in order to demonstrate that with the appropriate neural architecture, prediction of upcoming information (next-token prediction) is enough for an agent to build a cognitive map. These tasks are sequences of symbols with a hidden structure that the model must infer in order to generalize.

To validate the computational benefits of rotation matrices (that will never be total, see sec. 10.4) we would like our models to allow the learning of lower level structures such as gating, while correctly representing 2-dimensional space. To test this versatility, we started with a 1-dimensional gating structure as our baseline task (section 5.1), as it is the most basic structure that a model should be able to represent, and since current selective models such as Mamba and CoPE manage to solve it, so should *MapFormers*. We then tested *MapFormers* on grid navigation, first in 1D, to show that even 1-dimensional structures are more than gating, and later in 2D, because it is the historical task [11, 12, 13] and the most fundamental cognitive map to learn for an agent evolving in the physical world, and its *irreducible representations* are rotations that cannot be learned with the diagonal matrices of models listed above, which should demonstrate the superiority of *MapFormers*.

5.1 Selective copy

In this task introduced in sec. 3.1, the model receives a sequence of symbols and must copy it entirely while ignoring a blank token B : $CFEABABBCBF \rightarrow CFEAACF$, which requires the model to learn a gating mechanism to ignore blank tokens. OOD sequences are generated by varying the proportion of blank tokens. Our training sequences have 128/128 non blank/blank tokens, OOD

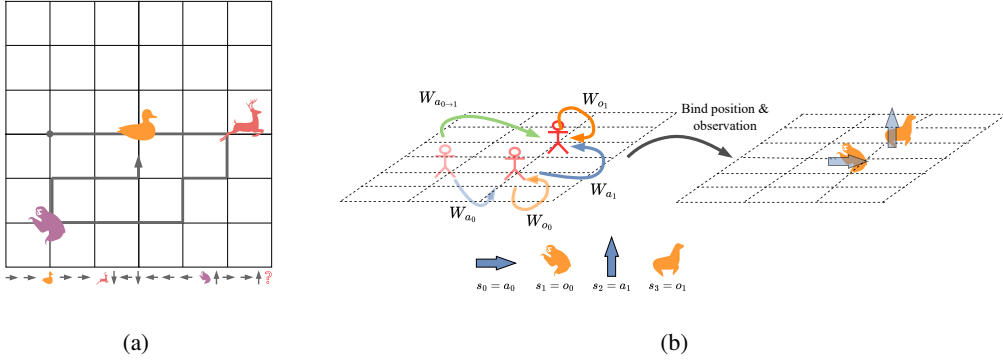


Figure 3: **The 2D-Navigation Task and an Illustration of the Desired Corresponding Cognitive Map.** (a) Illustration of the 2D navigation task: A model must predict the upcoming observation every time it comes back to it. The model only receives symbols, and must make sense of them without supervision. Some represent observations, others actions to take. (b) To solve this task, only actions (blue) should update the cognitive map, while observations (orange) leave it untouched. That is, observations should be projected to zero integration times. The logic is reversed for content, which is only updated by observation tokens, while actions are projected to zero (shaded blue). That is, value vectors of actions should be close to zero.

Dense 128/64 and OOD sparse 128/256. For this task, we follow the training setup of [26] and train models with 2 layers, 4 heads of size 64.

	IID	OOD Dense	OOD Sparse
<i>MapEM-o</i>	0.11	0.08	0.07
<i>MapEM-s</i>	0.10	0.11	0.10
RoPE	1.0	0.48	0.22
CoPE	1.0	1.0	1.0
MapWM	1.0	1.0	1.0
MapEM-os	1.0	1.0	1.0

Table 1: **Selective copy accuracy.** IID sequences are generated with 128 tokens to copy and 128 blank tokens B to ignore. OOD-d (dense) and OOD-s (sparse) vary the amount of blank tokens to ignore to 64 and 256, respectively. RoPE solves the task IID but fails to generalize OOD, while as expected, both CoPE and *MapFormer* can solve it, showing that the latter can also learn gating mechanisms. *MapEM-o* and *MapEM-s* cannot solve this task, since it requires both "sensory" inputs (the tokens to copy) and structure (the tokens to ignore).

In line with [26], we find that RoPE perfectly learns in distribution but completely fails to generalize, while as expected, both CoPE and our models manage to solve the task on OOD samples, since moving forward on a finite segment or a circle are equivalent. Because this task involves copying relevant tokens, it cannot be solved without sensory inputs (the token to copy), and therefore *MapEM-s*, our model relying on structure alone, cannot solve it.

5.2 Forced Grid Navigation

An agent evolving in a two-dimensional world should understand how coordinates combine in order to keep track of its position. Our task consists of a random sequence of symbols $s = (a_1, o_1, a_2, o_2, \dots, a_T, o_T)$ with action a_t sampled from $\{\uparrow, \downarrow, \rightarrow, \leftarrow\}$ and observation o_t from $\{o_1, \dots, o_K\}$, a finite set of K objects, plus a blank token B to ignore. Every time the agent comes back to a previously visited location $p_t = p_s, s < t \leq T$, it is asked to recall the last object o_s it has seen there (fig. 3a).

	1D navigation			2D Navigation		
	IID	OOD-d	OOD-s	IID	OOD-d	OOD-s
<i>MapEM-o</i>	0.14	0.20	0.12	0.16	0.08	0.08
RoPE (1L)	0.24	0.39	0.16	0.33	0.35	0.29
RoPE (2L)	0.28	0.42	0.15	0.33	0.31	0.29
RoPE (4L)	0.20	0.31	0.11	0.33	0.32	0.28
CoPE (1L)	0.58	0.74	0.42	0.66	0.74	0.59
CoPE (2L)	0.67	0.74	0.57	0.63	0.72	0.52
CoPE (4L)	0.72	0.83	0.62	0.67	0.73	0.57
<i>MapWM</i>	1.0	1.0	1.0	0.99	0.99	0.96
<i>MapEM-os</i>	1.0	1.0	1.0	1.0	0.99	0.97
<i>MapEM-s</i>	1.0	1.0	1.0	1.0	1.0	0.99

Table 2: **1D-2D grid navigation accuracy.** RoPE does not solve the task since it does not learn input-dependent matrices. CoPE performs better but does not solve the task, even in 1D, showing that gating is not enough to learn 1D cognitive maps, since it does not allow to learn the inverse of an action (forward/backward). Even with up to 4 layers, both RoPE and CoPE fail to solve the task, showing that without the appropriate structure, deeper models cannot learn a cognitive map. All *MapFormers* model solved the task and perfectly generalize OOD, even if performances slightly degrade in 2D on longer sequences (OOD-s), since the amount of coordinates to represent increases quadratically. As expected *MapEM-o*, a transformer with no positional embeddings, performs even worse than RoPE, since it does not encode position.

In navigation tasks, we train all models on sequences of $l = 128$ steps, $p_{empty} = 0.5$ and a grid size of $l_{grid} = 64$ and test length generalization on two OOD datasets - OOD-d: $l = 64, p_{empty} = 0.2, l_{grid} = 32$ and OOD-s: $l = 512, p_{empty} = 0.8, l_{grid} = 128$.

Because this task only requires recall of information, we hypothesize that one layer coupled with path integration should be enough, as in [22]. We set the inner rank r (see sec.4) of the integration time projection W_Δ to the world dimension n : $r := n = 1, 2$ in 1D and 2D, respectively. We trained single layer models with two heads of size $h = 64$ on 200K sequences, with AdamW optimizer [31], a linear learning rate decay, a base learning rate $lr = 3e^{-4}$, weight decay 0.05 and a batch size of 128 on a single GPU.

1D grid navigation We first tested our models on a 1D navigation task, which has a subtle difference with gating. Even though the underlying structure is 1-dimensional, the model must be able to move forward or backward – *i.e.* representing an action and its inverse – while gating only compresses the ordinal order and can only move forward. Therefore, we hypothesize that CoPE, which learns a gating structure, should not be able to solve this task. As expected, all *MapFormer* models solve the task, but both RoPE and CoPE fail (tab. 2), showing a key limitation of gating even in 1D.

2D grid navigation As expected, our three model variants perfectly solve the task in 2D and generalize it to shorter or longer sequences. Even though CoPE does significantly better than RoPE, it fails to reach a perfect accuracy on both IID and OOD samples. Note that because 2D positions require more neurons to represent the two orthogonal axis, performances degrade faster on longer sequences than in 1D (tab. 2).

For both RoPE and CoPE, increasing the number of layers does not change the model’s performance, even though CoPE seems to benefit from more layers in 1D, probably because it helps the model to learn a backward operation that cannot be approximated with a single layer. Nevertheless, these results suggest that structure cannot be approximated with deeper networks without the appropriate inductive bias.

For pedagogical reasons, we added a control *MapEM-o*, a transformer with observation only, and as expected, the model does not learn anything, showing that structure is indeed learned through input-dependent positional encoding.

These results show the importance of learning input-dependent positional encoding in order to solve structure-dependent tasks with Transformers. CoPE, which only learns a gating mechanism, can solve the Selective Copy task but fails to learn a cognitive map, compared to *MapFormers* that perfectly generalize OOD in all tasks, demonstrating the expressive power of input-dependent matrices to solve structure-dependent problems.

5.3 EM is computationally more expensive but scales better than WM

Compared to *MapFormer-WM*, *MapFormer-EM* queries its memories with the flattened conjunction of observational and structural features, which requires a second pool of neurons $p_t \in \mathbb{R}^d$ as well as computing two attention matrices A_X and A_P separately. This offers sparser and higher dimensional features $g_t = \text{vec}(x_t.p_t^\top) \in \mathbb{R}^{d^2}$ (fig. 1c) but doubles the computational load of the attention operation, which is already the main bottleneck in scaling transformers.

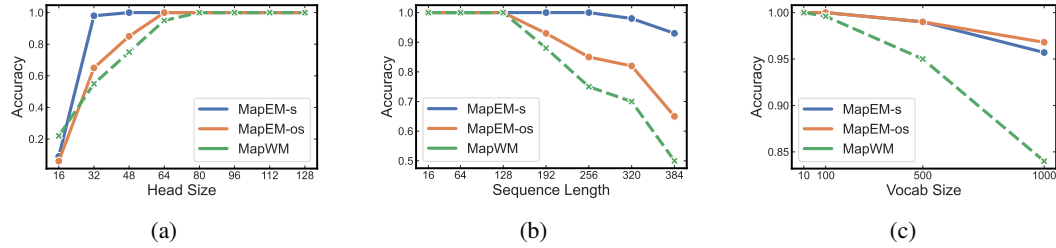


Figure 4: **Behavioral Analyses: MapEM scales better than MapWM** (a) Fixed sequence length $l = 256$, varying head size. (b) Fixed head size $h = 48$, varying sequence length. EM models are more robust to number of neurons and sequence length. (c) Fixed head size $h = 32$ and sequence length $l = 16$. Increasing the number of items to remember makes the task harder. Working memory models require more neurons to remember a large number of items.

This factorization in two separate pool of neurons should allow EM to be more efficient than WM, as in the former, neurons specialize for either position or observation. To verify our claim, we start by varying the number of neurons per head, to validate that *MapEM* models need less neurons, and in the same logic, we fix the model size but vary the sequence length to demonstrate that EM models represent positions with more precision. Finally, we decided to fix everything but vary the number of objects seen in training, to show that structure and memorization influence each other.

To test the impact of model size and sequence length, we vary the head size from 16 to 128 and sequence length from 16 to 384, respectively, while keeping a small vocabulary size of 10. To test the impact of vocabulary on recall, we varied the number of objects from 10 to 10000, and train small models with head size 32 on short sequences of size 16. Results are reported in fig. 4

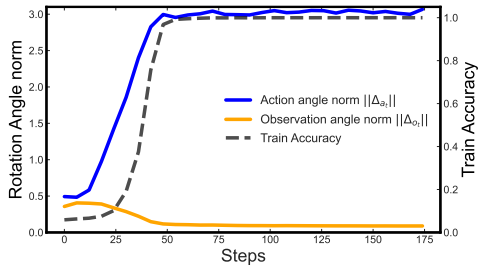
In line with [2], EM models scale better than WM, and unsurprisingly, our model relying on position alone (*MapEM-s*, blue) is more robust to both sequence length (fig. 4a) and model size (fig. 4b), since sensory features only add noise on this task. We clearly see here that the right architecture without enough neurons will completely fail to learn a cognitive map, highlighting the key role that model’s size plays in the ability to understand the structure of the world the agent evolves in.

The same effect is observed in memorization (fig. 4c), where WM models struggle to disambiguate objects when there are too many of them during training, while EM – which have a dedicated neural population for it – scale much better.

These experiments demonstrate the superior capacity of *MapEM* models in recall tasks, at the cost of doubling the attention computation.

5.4 Observations are vectors, actions are matrices

In our tasks, some symbols (actions $s_t = a_t \in \{\uparrow, \downarrow, \rightarrow, \leftarrow\}$) must update the model’s cognitive map (**where**), while others should leave it untouched (observations $s_t = o_t$), but modify its content (**what**). Since the choice of symbols is arbitrary, the model must learn by itself which ones are actions and which ones are observations. In order to demonstrate that the model has learned a cognitive map, we compare the learned representations of action *versus* observation tokens of our *MapFormer* models in the 2D Forced Navigation task. To demonstrate that the model has learned that only action tokens a_t modify the cognitive map, we first compared the learned action representations $\Delta_t^{in} \in \mathbb{R}^2$ and

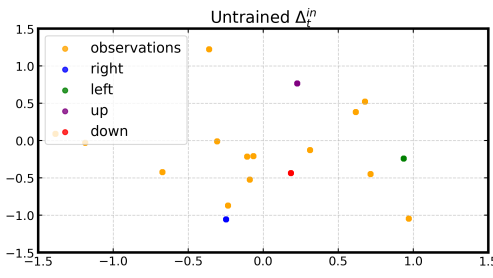


(a)

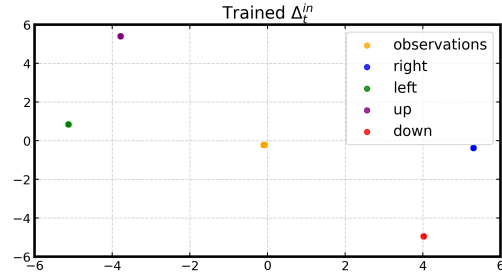
	right	left	up	down
right	1.0	-1.0	-0.6	0.7
left	-1.0	1.0	0.7	-0.8
up	-0.6	0.7	1.0	-1.0
down	0.7	-0.8	-1.0	1.0

	v_o_t	v_a_t
untrained	1.3	1.2
trained	18.2	3.1

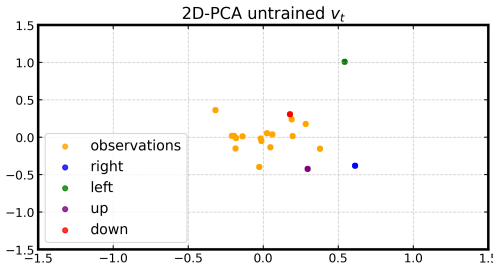
(b)



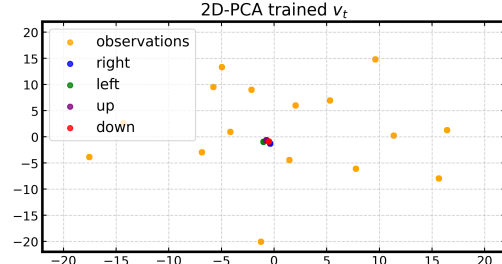
(c)



(d)



(e)



(f)

Figure 5: Neural Analyses: Actions are Matrices and Observations are Vectors: (a) Rotation angle norm $||\theta_t||$ vs Accuracy through training. Model reaches perfect accuracy as soon as it learns that action symbols a_t update the agent’s position while observation tokens o_t leave it untouched via 0-angle rotations, i.e. $R_{\theta_o} \approx \mathbf{I}_n$ (b) (top table) Action’s inner action $\Delta_{a_t}^{in}$ cosine similarities. Opposite actions (right v left / up v down) cancel each other ($\cos(\Delta_{left}^{in}, \Delta_{right}^{in}) = -1$), but orthogonal dimensions are not projected onto orthogonal axes ($|\cos(\Delta_{left}^{in}, \Delta_{up}^{in})| \gg 0$), implying that other constraints like [32] could be added to force disentanglement. (bottom table) Once trained, the norm of value embeddings v_t in the attention layer becomes much bigger for observations than actions ($||v_{o_t}|| \gg ||v_{a_t}||$), implying that only observations contribute in updating the state’s content. (c) Untrained model project observations and actions randomly (d) After training, observation tokens $s_t = o_t$ are all projected towards 0 (orange), while tokens representing opposite directions (left / right or up / down) are all projected to opposite directions. (e) Untrained model project values v_t randomly. (f) Trained model learns to ignore action’s content: $v_{a_t} \approx 0$.

$\Delta_t \in \mathbb{R}^{n_h \times n_b}$, since they define how the cognitive map must be updated. We also compared the representations of opposite actions (left/right and up/down), to verify that they cancel each other, as predicted by our theory. Finally, we also analyzed the learned value embeddings v_t to demonstrate that only observation tokens change the state’s content.

It’s exactly what we observe in fig. 5a, where perfect generalization is achieved as soon as the model learns that action tokens a_t trigger state rotation while observation tokens o_t leave it untouched: $\forall t, \Delta_{a_t} \gg \Delta_{o_t}$. Once trained, opposite actions (left / right or up / down) cancel each other (tab. 5b-

top), while observations are all projected to a zero angle (fig. 5d). If actions update the cognitive map, observations are the only ones to update the state’s content, since $||v_{o_t}|| \gg ||v_{a_t}||$ (fig. 5d-bottom & fig. 5f). In other words, actions are represented within the Lie algebra / action space \mathfrak{g} , while observations v_t belong to the *content space*, the traditional latent space of transformers.

Therefore, in *MapFormers*, actions are matrices and observations are vectors, which resembles the ideas presented in [33], where nouns are vectors and adjectives are matrices, giving the model stronger OOD generalization compared to baseline models. Given the fact that Transformers are a generic architecture that can be used for language modeling, it is more than likely that the action/observation separation will focus on functional/content words, creating a separation between adjectives and verbs represented in the Lie algebra \mathfrak{g} and nouns embedded in the content’s space.

Finally, the fact that observations o_t do not update the cognitive map ($\Delta_{o_t} \approx 0$) and actions do not change its content ($v_{a_t} \approx 0$) implies that at each time step t , the model *binds* o_t and a_t together within the cognitive map and the content’s space, with position p_t defined by a_t and the updated value’s content v'_t by o_t . To give a better intuition, in *MapEM*-s – which uses position only to compute attention – attention updates value v_t with a weighted sum of other values $v_{s \leq t}$ based on their structural similarity A_P . Since o_t does not update the cognitive map, we have $p_{o_t} = R_{\theta_{o_t}} p_{a_t} \approx p_{a_t} := p_t$, implying that their attention scores will be roughly equal. For the sake of simplicity, let us suppose that their similarity to other tokens in the sequence is null, meaning that $v'_{a_t} = (v_{o_t} + v_{a_t})/2$ and $v'_{o_t} = (v_{o_t} + v_{a_t})/2$. Because $v_{a_t} \approx 0$, we have $v'_{o_t} = v'_{a_t} = v_{o_t}/2 := v'_t$. This means that *MapFormers* have the ability to flexibly group structurally similar tokens together (tokens o_t and a_t for all time steps t , fig.3b).

All these results are compelling evidence that our models have indeed learned to represent actions, and therefore a cognitive map.

6 Discussion

We introduced *MapFormers*, a novel class of Transformer-based architectures designed to learn cognitive maps and perform parallel path integration in a fully self-supervised setup. Our approach addresses the key limitation of previous RNN-based models by leveraging the parallel processing ability of Transformers, which is essential for scaling to complex, long-sequence problems. We developed two variants, the *MapFormer-WM* (Working Memory) and *MapFormer-EM* (Episodic Memory), which unify relative and absolute positional embeddings, respectively, as computational models of these distinct memory systems. Critically, we extended the theoretical framework of actionable representations [27], drawing on Lie-group theory, to enable this efficient, parallel path integration for large-scale structure learning.

Modern AI systems struggle with Out-of-Distribution (OOD) generalization and require orders of magnitude more data to achieve performance on par with humans. This limited OOD generalization can be explained by a misrepresentation of the true structure underlying the train and test data, suggesting that extracting and representing this structure in the form of a cognitive map offers a potential remedy. In our experiments, we found that *MapFormers* achieve almost perfect generalization to longer and sparser sequences, significantly outperforming baseline models. For problems that required only simple gating capabilities, *MapFormers* and models using CoPE [26] achieved similar OOD generalization, as expected; however, for more complex problems which require the creation of a cognitive map, only *MapFormers* successfully generalized OOD. This demonstrates the important role of *input-dependent* positional encoding — endowed with the appropriate group structure — for structure-based OOD generalization, distinguishing it from generalization that might merely rely on sophisticated heuristics.

The key difference between EM and WM models comes from the explicit *versus* implicit representation of structure [2]. In EM models, memories are formed by the conjunction of position and content, increasing the dimensionality of the representational space by a quadratic factor compared to WM models (as illustrated and reflected by the size of the final state in fig 1c & 1d). This specialization of neurons allows EM model to scale better, being more robust to model size, sequence length and vocabulary size (fig. 4).

How to know whether *MapFormers* have indeed learned a cognitive map? We identified several behavioral and neural evidences for that: First, the location in a cognitive map should be affected only by actions and not by content tokens (observations). fig. 5a shows that, indeed, once the model has

learned that only actions should trigger rotations while observations should not, perfect generalization was achieved. Second, in a cognitive map, opposite actions (such as ‘step left’ vs. ‘step right’) should cancel each other. Indeed, fig. 5b and fig. 5d shows that the integration times (the coefficients of the representations of the actions in the Lie algebra) have opposite signs, and therefore would sum up to zero. Third, just as content tokens should not affect position in the cognitive map, actions should not have a ‘sensory’ content. Indeed, fig. 5f shows that the value vectors V ’s of actions are an order-of-magnitude smaller than that of content observation tokens. Together, this shows that *MapFormers* learn to tell apart actions from observations, such that only actions affect the neural population that encode position in a cognitive map, with opposite effects for opposite actions, and only observations enter into content representation while actions have a negligible effect, allowing *MapFormers* to *bind* the position and content of structurally similar tokens. In other words, in *MapFormers*, observations are vectors and actions are matrices; *MapFormers* learn two distinct latent neural spaces: (1) a space that represents content (as in traditional deep learning models), and (2) a space that represents abstract actions in low dimension, within the Lie algebra (fig.1).

MapFormers overcome the computational bottleneck of previous RNN-based EM/WM models [2, 17, 22], delivering efficiency and scalability comparable to standard Transformers. The main bottleneck of EM/WM RNNs is their slow processing time, but *MapFormers* require little extra compute compared to baseline Transformers. For problems that can be addressed with rotational operation, using 2×2 rotation matrices allowed us to avoid computing a matrix exponential and matrix-vector products (eq. 18), while remaining compatible with *FlashAttention* for *MapWM* models. Our experiments show the effectiveness of *MapFormers*, trained on significantly longer sequences than those explored in previous work [2].

Compared to previous *actionable* models [2, 17, 22], using matrix exponential to learn input-dependent matrices allows us to analyze sequence processing models through Lie-group theory. This framework is useful to better characterize the type of structures that are learnable by the model. Furthermore, *MapFormers* provide greater flexibility compared to previous actionable models because they eliminate the need to assume the underlying structure. For instance, prior models required either the explicit knowledge of the number of possible actions or the irreducible matrix representations (the irreps) of the underlying group structure, which is often a prohibitive requirement in most applications.

The exponential map – needed to learn input-dependent matrices and therefore cognitive maps – arises in discrete SSMs via the integration of infinitesimal recurrent changes over a varying time interval. This explains how a model with fixed synaptic connections A can learn a cognitive map by just varying the duration at which it exposes the input to neural transformations, giving rise to the matrix $\bar{A}_t := \exp(\Delta_t A)$ (eq. 8), indicating that the neural mechanisms allowing animals to build cognitive maps is easier than we might think, since it naturally emerges in continuous, selective recurrent networks.

The Transformer architecture is generic; it has been used in a variety of different tasks from language modeling to vision and protein folding [34, 35]. The mechanism for learning a cognitive map, as our formalism shows, is also generic. The combination of the two in *MapFormers* suggests that non-spatial cognitive maps can thus be learned in a variety of different tasks. For example, in the case of language modeling, learning a cognitive map would mean disentangling the structure of sentences (syntax) from their content (semantics).

While in this work we explored with only rotation matrices, for computational efficiency, more complex group structures (including non-commutative) can be learned by *MapFormers*. This might affect inference speed, making a tradeoff between expressibility and computing time (sec. 10.4).

7 Limitations

We highlight several limitations of our work that we left for future explorations. First, in order to compute *path integration*, we sum the rotation angles along the temporal dimension, meaning that our formalism only applies to causal transformers. Further work is needed to generalize our method to non-causal problems such as image processing, but the same methods used to adapt SSMs to vision [36] could be used. Second, we did not try to scale our method to larger model sizes and larger datasets, but since *MapFormers* require little extra compute compared to baseline transformers, computation time should not be a bottleneck. Third, our results only confirm the superiority of EM models on recall tasks compared to their WM counterparts, but further experiments should compare

these two models on more complex tasks that involve reasoning. Finally, in our models, for numerical efficiency, we only use block diagonal matrices, without orthogonal matrix M used in eq.2, since orthogonal matrices do not change the value of a scalar product and should have no impact on the attention. However, real neurons cannot have a negative firing rate, and because of that, position p_t must always be positive, which is impossible with a block diagonal rotation matrix. Matrix M mixes frequencies together to make the code non negative [27], which creates a fundamental difference between our models and biological systems. Non-negativity and bounded activity can also result in disentangled representations [32], which could help build even more robust and interpretable cognitive maps in the future.

8 Conclusion

We introduce simple theoretical arguments from Lie-group theory to analyze transformers and SSMs, allowing us to characterize the type of structures that these models are able to learn, and show that diagonal matrices used in current SSMs are not expressive enough to learn spatial cognitive maps. From this, we introduce *MapFormer*, which generalizes the Transformer architecture with input-dependent transformations, and unify relative and absolute positional embeddings with computational models of working and episodic memory, respectively. Our models leverage the parallel sequential processing ability of Transformers to compute path integration in parallel, mandatory for larger-scale applications, and with a minimal structural bias, learn a cognitive map within their positional embeddings via prediction of upcoming observations. *MapFormers* are, to the best of our knowledge, the first to learn such maps without any supervision and learn to represent actions as invertible matrices, facilitating generalization by ensuring a consistent application of these actions across samples, while increasing explainability via a direct access to the sequence of actions taken by the model.

This work has implications in both neuroscience and AI: for the former, it explains the neural mechanisms giving rise to cognitive maps; in machine learning, this work allows to learn structure and relations at scale, creating smaller, more robust and interpretable models.

9 Acknowledgments

This work has benefited from public funding from the IA-Cluster PR[AI]RIE-PSAI project, managed by the French National Research Agency (ANR) as part of the France 2030 program, reference “ANR-23-IACL-0008”. Ecole Normale Supérieure-PSL’s Département d’Etudes Cognitives is supported by ANR grants, ANR-10-IDEX-0001-02 and FrontCog, ANR-17-EURE0017.

References

- [1] Richard J. Gardner, Erik Hermansen, Marius Pachitariu, Yoram Burak, Nils A. Baas, Benjamin A. Dunn, May-Britt Moser, and Edvard I. Moser. Toroidal topology of population activity in grid cells. *Nature*, 602(7895):123–128, Feb 2022.
- [2] James C.R. Whittington, William Dorrell, Timothy E.J. Behrens, Surya Ganguli, and Mohamady El-Gaby. A tale of two algorithms: Structured slots explain prefrontal sequence memory and are unified with hippocampal cognitive maps. *Neuron*, 113(2):321–333.e6, Jan 2025.
- [3] Ashish Vaswani, Noam Shazeer, Niki Parmar, Jakob Uszkoreit, Llion Jones, Aidan N Gomez, Łukasz Kaiser, and Illia Polosukhin. Attention is all you need. In I. Guyon, U. Von Luxburg, S. Bengio, H. Wallach, R. Fergus, S. Vishwanathan, and R. Garnett, editors, *Advances in Neural Information Processing Systems*, volume 30. Curran Associates, Inc., 2017.
- [4] Sébastien Bubeck, Varun Chandrasekaran, Ronen Eldan, Johannes Gehrke, Eric Horvitz, Ece Kamar, Peter Lee, Yin Tat Lee, Yuanzhi Li, Scott Lundberg, Harsha Nori, Hamid Palangi, Marco Tulio Ribeiro, and Yi Zhang. Sparks of artificial general intelligence: Early experiments with gpt-4, 2023.
- [5] Meredith Ringel Morris, Jascha Sohl-dickstein, Noah Fiedel, Tris Warkentin, Allan Dafoe, Aleksandra Faust, Clement Farabet, and Shane Legg. Levels of agi for operationalizing progress on the path to agi, 2024.
- [6] Keyon Vafa, Justin Y. Chen, Ashesh Rambachan, Jon Kleinberg, and Sendhil Mullainathan. Evaluating the world model implicit in a generative model, 2024.
- [7] Sean Williams and James Huckle. Easy problems that llms get wrong, 2024.
- [8] Tom McCoy, Ellie Pavlick, and Tal Linzen. Right for the wrong reasons: Diagnosing syntactic heuristics in natural language inference. In Anna Korhonen, David Traum, and Lluís Márquez, editors, *Proceedings of the 57th Annual Meeting of the Association for Computational Linguistics*, pages 3428–3448, Florence, Italy, July 2019. Association for Computational Linguistics.
- [9] Gregoire Deletang, Anian Ruoss, Jordi Grau-Moya, Tim Genewein, Li Kevin Wenliang, Elliot Catt, Chris Cundy, Marcus Hutter, Shane Legg, Joel Veness, and Pedro A Ortega. Neural networks and the chomsky hierarchy. In *The Eleventh International Conference on Learning Representations*, 2023.
- [10] Timothy E.J. Behrens, Timothy H. Muller, James C.R. Whittington, Shirley Mark, Alon B. Baram, Kimberly L. Stachenfeld, and Zeb Kurth-Nelson. What is a cognitive map? organizing knowledge for flexible behavior. *Neuron*, 100(2):490–509, 2018.
- [11] Edward C. Tolman. Cognitive maps in rats and men. *Psychological Review*, 55(4):189–208, 1948.
- [12] J. O’Keefe and L. Nadel. *The hippocampus as a cognitive map*. Clarendon Press, Oxford, United Kingdom, 1978.
- [13] Torkel Hafting, Marianne Fyhn, Sturla Molden, May-Britt Moser, and Edvard I. Moser. Microstructure of a spatial map in the entorhinal cortex. *Nature*, 436(7052):801–806, Aug 2005.
- [14] Dmitriy Aronov, Rhino Nevers, and David W. Tank. Mapping of a non-spatial dimension by the hippocampal–entorhinal circuit. *Nature*, 543(7647):719–722, Mar 2017.
- [15] Nikolaus Kriegeskorte and Katherine R. Storrs. Grid cells for conceptual spaces? *Neuron*, 92(2):280–284, 2016.
- [16] Seongmin A. Park, Douglas S. Miller, and Erie D. Boorman. Inferences on a multidimensional social hierarchy use a grid-like code. *Nature Neuroscience*, 24(9):1292–1301, Sep 2021.
- [17] James CR Whittington, Timothy H Muller, Shirley Mark, Guifen Chen, Caswell Barry, Neil Burgess, and Timothy EJ Behrens. The tolman-eichenbaum machine: Unifying space and relational memory through generalisation in the hippocampal formation. *bioRxiv*, 2019.

[18] H. Freyja Ólafsdóttir, Daniel Bush, and Caswell Barry. The role of hippocampal replay in memory and planning. *Current Biology*, 28(1):R37–R50, Jan 2018.

[19] Lorelei R. Howard, Amir Homayoun Javadi, Yichao Yu, Ravi D. Mill, Laura C. Morrison, Rebecca Knight, Michelle M. Loftus, Laura Staskute, and Hugo J. Spiers. The hippocampus and entorhinal cortex encode the path and euclidean distances to goals during navigation. *Current Biology*, 24(12):1331–1340, 2014.

[20] Rüdiger Wehner and Mandyam V. Srinivasan. Searching behaviour of desert ants, genus-*cataglyphis* (formicidae, hymenoptera). *Journal of comparative physiology*, 142(3):315–338, Sep 1981.

[21] Jianlin Su, Yu Lu, Shengfeng Pan, Ahmed Murtadha, Bo Wen, and Yunfeng Liu. Roformer: Enhanced transformer with rotary position embedding, 2023.

[22] James C.R. Whittington, Joseph Warren, and Timothy E.J. Behrens. Relating transformers to models and neural representations of the hippocampal formation, 2022.

[23] Hubert Ramsauer, Bernhard Schäfl, Johannes Lehner, Philipp Seidl, Michael Widrich, Thomas Adler, Lukas Gruber, Markus Holzleitner, Milena Pavlović, Geir Kjetil Sandve, Victor Greiff, David Kreil, Michael Kopp, Günter Klambauer, Johannes Brandstetter, and Sepp Hochreiter. Hopfield networks is all you need, 2021.

[24] Albert Gu and Tri Dao. Mamba: Linear-time sequence modeling with selective state spaces, 2024.

[25] Tri Dao and Albert Gu. Transformers are ssms: Generalized models and efficient algorithms through structured state space duality, 2024.

[26] Olga Golovneva, Tianlu Wang, Jason Weston, and Sainbayar Sukhbaatar. Contextual position encoding: Learning to count what’s important, 2024.

[27] William Dorrell, Peter E. Latham, Timothy E. J. Behrens, and James C. R. Whittington. Actionable neural representations: Grid cells from minimal constraints, 2023.

[28] Anthony W Knapp and Anthony William Knapp. *Lie groups beyond an introduction*, volume 140. Springer, 1996.

[29] Albert Gu, Karan Goel, and Christopher Ré. Efficiently modeling long sequences with structured state spaces, 2022.

[30] Sinong Wang, Belinda Z. Li, Madian Khabsa, Han Fang, and Hao Ma. Linformer: Self-attention with linear complexity, 2020.

[31] Ilya Loshchilov and Frank Hutter. Decoupled weight decay regularization, 2019.

[32] James C. R. Whittington, Will Dorrell, Surya Ganguli, and Timothy E. J. Behrens. Disentanglement with biological constraints: A theory of functional cell types, 2023.

[33] Marco Baroni and Roberto Zamparelli. Nouns are vectors, adjectives are matrices: Representing adjective-noun constructions in semantic space. In Hang Li and Lluís Márquez, editors, *Proceedings of the 2010 Conference on Empirical Methods in Natural Language Processing*, pages 1183–1193, Cambridge, MA, October 2010. Association for Computational Linguistics.

[34] John Jumper, Richard Evans, Alexander Pritzel, Tim Green, Michael Figurnov, Olaf Ronneberger, Kathryn Tunyasuvunakool, Russ Bates, Augustin Žídek, Anna Potapenko, Alex Bridgland, Clemens Meyer, Simon A. A. Kohl, Andrew J. Ballard, Andrew Cowie, Bernardino Romera-Paredes, Stanislav Nikolov, Rishabh Jain, Jonas Adler, Trevor Back, Stig Petersen, David Reiman, Ellen Clancy, Michal Zieliński, Martin Steinegger, Michalina Pacholska, Tamas Berghammer, Sebastian Bodenstein, David Silver, Oriol Vinyals, Andrew W. Senior, Koray Kavukcuoglu, Pushmeet Kohli, and Demis Hassabis. Highly accurate protein structure prediction with alphafold. *Nature*, 596(7873):583–589, Aug 2021.

- [35] Oriane Siméoni, Huy V. Vo, Maximilian Seitzer, Federico Baldassarre, Maxime Oquab, Cijo Jose, Vasil Khalidov, Marc Szafraniec, Seungeun Yi, Michaël Ramamonjisoa, Francisco Massa, Daniel Haziza, Luca Wehrstedt, Jianyuan Wang, Timothée Darcet, Théo Moutakanni, Leonel Sentana, Claire Roberts, Andrea Vedaldi, Jamie Tolan, John Brandt, Camille Couprie, Julien Mairal, Hervé Jégou, Patrick Labatut, and Piotr Bojanowski. Dinov3, 2025.
- [36] Lianghui Zhu, Bencheng Liao, Qian Zhang, Xinlong Wang, Wenyu Liu, and Xinggang Wang. Vision mamba: Efficient visual representation learning with bidirectional state space model, 2024.

10 Appendix

10.1 **MAMPa**: Mamba with skew-symmetric block-diagonal matrices

As explained in sec.3.5, one only needs to modify the recurrent matrix $A := S = -S^\top$ of selective SSMs to be block-diagonal skew-symmetric in order to learn spatial cognitive maps. However, the reason why people chose diagonal matrices in Mamba is to dramatically reduce the inference speed of these models, and make them as close as possible to parallelized. In Mamba, an efficient implementation of the parallel scan is used, leveraging the fact that A is diagonal and can therefore be treated as a vector. Even then, the author reduce the internal state to $N = 16$, which has a dramatic impact on the ability to learn cognitive maps, as demonstrated in fig. 4. In Mamba2, the authors go even further by choosing $A := a \in \mathbb{R}$ to be a scalar, which allows them to broadcast it easily in the attention matrix and increase the state size to $N = 64$ (eq. 16).

However, as we have demonstrated in our experiments, diagonal matrices are not expressive enough to learn spatial cognitive maps, nor any other higher dimensional map. We implemented a parallel scan on square matrices to test if **MAMPa**, an extended version of Mamba with 2×2 block-diagonal matrices can learn spatial maps like our theory predicts. Because the parallel scan on bigger matrices dramatically increases the computational load, we were forced to keep the inner state small ($N = 16$) and only trained models on sequences of size $l = 16$. We report the results in tab. 3, where OOD dense and OOD sparse use sequences of size 8 and 32 respectively.

	IID	OOD-d	OOD-s
Mamba	0.42	0.77	0.40
MAMPa	0.74	0.93	0.60
<i>MapWM</i>	1.0	1.0	1.0
<i>MapEM-os</i>	1.0	1.0	1.0
<i>MapEM-s</i>	1.0	1.0	1.0

Table 3: **SSM 2D grid navigation - Accuracy.** As expected, *MaMPA* offers substantial improvements over Mamba, but fails to reach performances a par with *MapFormers*, while being slower.

This confirms that our formalism extends to SSMs, but also shows that what has allowed the scaling of selective SSMs – diagonal matrices to reduce the computational load – is what prevents them from learning cognitive maps, leaving only transformers as scalable implementations of structure learning models.

10.2 Frequency initialization

Like *grid cells* that fire at different frequencies [13], our formalisms uses rotations at different scales, scale whose initialization has a major impact on position representations.

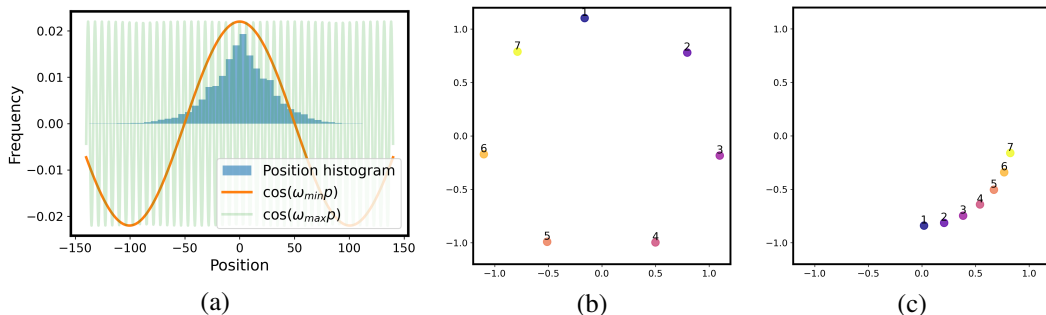


Figure 6: (a) Distribution histogram of position in 1D navigation vs oscillation at the highest (green) and lowest (orange) frequencies. The longest distances reached by the model are comparable with the length of ω_{\min} cycles.(b-c) Rotation blocks at high and low frequencies.

The highest frequency ω_{\max} defines the finest granularity $\Delta_{\min} = \frac{2\pi}{\omega_{\max}}$ at which the signal is encoded, while low frequencies encode long range dependencies. We would like the lowest frequency

$\omega_{min} := \frac{2\pi}{\Delta_{max}}$ to complete its cycle once the the model has covered the longest distance Δ_{max} it possibly can, where $\Delta_{max} = n$ on a n -size grid (fig. 6).

Frequencies should encode signal at different scales, and a geometric initialization like the one used in RoPE [21] spreads the scales uniformly between 1 and $\Delta_{min} = \frac{1}{base}$ with:

$$\omega_i = \left(\frac{1}{\Delta_{max}} \right)^{-\frac{i}{n_b}}, \quad 1 \leq i \leq n_b$$

where $base \approx 10000$ in RoPE, dictates how many tokens the model has to see before completing a full circle. Compared to RoPE that always rotates by a constant angle $\Delta = 1$, our input-dependent angles Δ_t can take values bellow 1, and as such we might want our highest frequency ω_{max} to be greater than 1. We extend the logic such that:

$$\forall i : \omega_i = \omega_{max} \left(\frac{1}{\Delta_{max}} \right)^{-\frac{i}{n_b}} \implies \begin{cases} \omega_{max} = \frac{2\pi}{\Delta_{min}} \\ \omega_{min} = \frac{\omega_{max}}{\Delta_{max}} = \frac{2\pi}{n} \\ \implies \Delta_{max} = \frac{n \times \omega_{max}}{2\pi} \end{cases} \quad (19)$$

Leaving only ω_{max} and $base := n$ as hyperparameter-parameters and find that initializing $1 < \omega_{max} \leq 2\pi$ to work well in practice.

10.3 3D and 5D navigation

Because translations in n dimensions are just n independent 1D-translations on orthogonal axes, our models should theoretically be able to track position on these structures – with rotation blocks representing movement on one specific dimension – but should require a higher number of neurons to represent movement on all these orthogonal axes.

We train all models with a head size of 64. In 3D, we choose a sequence length of 256 and a grid size of 16. The task being particularly hard in 5D, we decided to reduce the sequence length to 16 and the grid size to 5 and report the results in tab. 4.

	3D navigation			5D Navigation		
	IID	OOD-d	OOD-s	IID	OOD-d	OOD-s
RoPE (1L)	0.39	0.36	0.35	0.74	0.45	0.33
CoPE (1L)	0.78	0.82	0.74	0.94	0.80	0.69
MapWM	1.0	0.95	0.94	0.75	0.50	0.35
MapEM-os	1.0	0.99	0.99	1.0	0.98	0.84
MapEM-s	1.0	1.0	0.98	1.0	1.0	0.87

Table 4: **3D - 5D grid navigation accuracy.** 2×2 block-diagonal rotation matrices can represent translations in 3D and 5D, since it equivalent to (3 or 5) 1D orthogonal translations. However, performances quickly degrade, since the amount of positions to represent grows exponentially. Notably, in 5D, **MapWM** fails to learn the task and perform a par with RoPE, while **MapEM**, which scale better in recall tasks, solve it even though performances start to degrade on longer sequences.

As we can see, all of our models converge in dimension 3, confirming that 2D-rotations are enough to learn simple translations in higher dimension. However, our WM models never manage to learn a cognitive map in 5D, and actually performances comparable to RoPE and much worse than CoPE, showing once again the increased robustness of EM models on recall tasks. Note that in 5D, because we keep the world size and sequence length small, CoPE asymptotically approaches a perfect score on the training set but fails to generalize OOD, while EM models solve it with 6 times less training data and generalize, highlighting the difference between learning of a cognitive map versus statistical heuristics. Models learning a cognitive map achieve robust generalization with much fewer data points, something that has been observed when comparing learning efficiency in humans versus AI models.

10.4 Groups beyond 2D rotations

So far, all our experiments were run with 2×2 block-diagonal matrices, which we demonstrated in section 10.3 to be enough to capture translations in higher dimensions, as rotations on orthogonal circles. However, it is unlikely that the brain performs perfect rotations, and a model should be able to converge to the desired matrix representation. In this section, we decided to explore matrices beyond 2×2 rotations, and analyze the tradeoff between model's expressivity and inference speed. We will start by analyzing the impact of increasing the block size of our rotation matrices, as well as changing their structure, to not be skew-symmetric anymore. Finally, we will analyze non-commutative group structures, and show that they can be learned, at the cost of losing parallel sequence abilities.

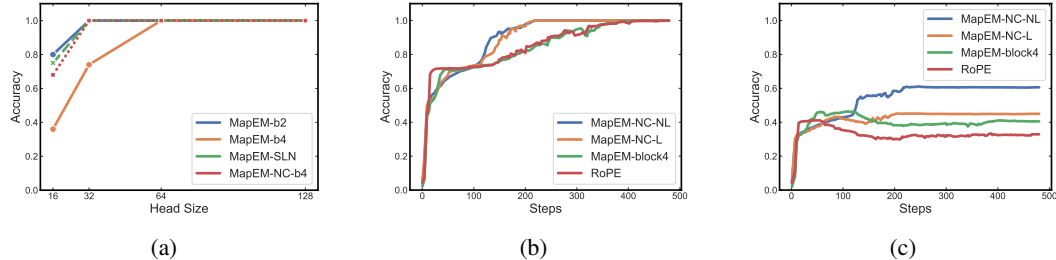


Figure 7: **Influence of matrix structure, block size and non-commutativity on the ability to learn cognitive maps.** (a) All models were trained on sequences of length 128. *MapEM* performances drop significantly when varying block size from 2 (blue) to 4 (orange) since it reduces the amount of learned rotations. Having a non commutative model of size 4 (red) allows to flexibly switch between rotations on each blocks, and keep performances competitive with blocks 2. Other group structures like $SL(2, n)$ can also be used (*MapEM-SLN*, green). (b-c) Navigation on 4D-rotations, needing non commutative matrices. We introduce *MapEM-NC-L* and *MapEM-NC-NL*, two non commutative variants of EM models, where θ_t are learned respectively via linear and non-linear functions. (c) Accuracy through training, where non-commutative reach a perfect accuracy early, while EM and RoPE approach it asymptotically. (d) Generalization to double sequence length. Only NC-NL manages not to drop in accuracy, showing the difficulty of learning a non-linear Lie algebra \mathfrak{g}

10.4.1 Other commutative groups

The first experiment that we conducted was to increase the block size of our rotation matrices. Since a single generator matrix S can only generate rotations along a single axis, we anticipate that using blocks of size $b > 2$ should be useless since it requires more neurons to perform a similar operation, and cannot benefit from the explicit formulation of matrix exponential (eq 2). It is what we observe in fig.7a, where *MapEM-b4*, EM model with blocks of size $b = 4$ (orange), needs twice the amount of neurons than *MapEM-b2* (blue).

Aside from block size, as Lie-group theory predicts, the nature of matrix A influences the learned structure. The special linear group $SL(n, \mathbb{R})$ – which preserves determinant, *i.e.* areas – can be represented using matrices with a null trace: $A = \bar{A} - \text{Tr}(\bar{A}) \implies \text{Tr}(A) = 0$. This group is more expressive than $SO(n)$ and in particular, we show that it can also be used to solve navigation tasks (fig. 7a, *MapEM-SLN*, block-size 2, green).

Finally, we tested *MapEM-NC*, a non-commutative model that we detail further in sec. 10.4.2. This model learns a basis of rotations per block S_i , $1 \leq i \leq K$, allowing it to switch rotation axes on the fly. We show that such a model with block size $b = 4$ and basis size $K = 6$ (red) performs a par with *MapEM-b2*, and much better than a model with the same block size but a single generator matrix S (*MapEM-b4*). This implies that what matters is the amount of rotations to perform rather than the block size in itself.

10.4.2 Non commutative Lie Groups

The ability to learn non commutative rules is fundamental, since rules as simple as "mother" and "father" should not commute. Indeed, the father of my mother is my grand father on my mother's side, while the mother of my father is my grand mother on my father's side, hence ending in a different position within the family tree/graph. This implies that the learned matrices do not commute, *i.e.*: $\mathbf{W}_{\text{mother}} \mathbf{W}_{\text{father}} \neq \mathbf{W}_{\text{father}} \mathbf{W}_{\text{mother}}$.

Compared to dimension 2 where a single 2×2 skew-symmetric matrix S is enough to generate any rotation, the basis of skew-symmetric matrices scales quadratically, since there are $n(n-1)/2$ ways to permute axis in dimension n , meaning that a single weight matrix will never be enough to encode all these rotation axis. Therefore, any rotation in $SO(n)$ must be expressed with a basis of $n(n-1)/2$ skew-symmetric matrices $\{S_i\}_{1 \leq i \leq K}$, matrices that do not commute together in general ($S_i S_j \neq S_j S_i$):

$$R_\theta^n = \exp \left(\sum_{i=1}^{n(n-1)/2} \theta_i S_i \right) \neq \prod_{i=1}^{n(n-1)/2} \exp(\theta_i S_i) \quad (20)$$

We see here that non-commutativity implies that path integration cannot be performed via the exponential of a sum anymore and can only be achieved via a sequential matrix product scaling linearly with sequence length L .

We introduce non-commutative models (NC), with a basis of $K = n(n-1)/2$ skew-symmetric matrices $\{S_i\}_{1 \leq i \leq K}$, $\theta := \Delta_t \omega \in \mathbb{R}^{n_h \times n_b \times K}$ and $R_\theta = \exp \left(\sum_{i=1}^K \theta_i S_i \right)$. The non commutativity forces us to compute path-integration sequentially and use a parallel scan to speed-up computation, since our models cannot leverage the parallel processing abilities of Transformers anymore, making them analogous to TEM-t [22], where path integration is computed sequentially before computing attention.

When the Lie group G is not commutative, the coordinates $\Delta_{t_i} \omega S_i$ do not add-up linearly, g becomes a curved manifold and cannot be treated as a vector space anymore. For that reason, we hypothesize that a linear mapping like we used in our *MapFormer* models should not capture the complexity of the group's manifold. Because of this, we introduce two non-commutative variants. (1) **MapEM-NC-L** with a linear mapping: $\Delta_t := W_\Delta x_t$ and (2) **MapEM-NC-NL** that uses an MPL to infer the rotation angles $\Delta_t := f_\Delta(x_t)$.

To validate our theory, we reproduce our navigation task, where this time actions represent 4D notations and not translations anymore, needing a non-commutative Lie algebra in order to be solved. The task being particularly hard, and our non-commutative models slow to train, we train our models on sequences of length 16, and test on length 32. We compare our models to RoPE and an *MapEM*-s with block size 4 in fig. 7b & 7c. As expected, our two EM-NC model solve the task faster, while EM and RoPE reach a perfect accuracy asymptotically, implying that they probably memorized the training dataset. However, only our non-commutative model with a non-linear mapping (*MapEM-NC-NL*) has non-degrading performances on the OOD dataset (fig 7c, blue), but still far from perfect accuracy. This highlights the importance of learning non-commutative rotations, but also how difficult it is to approximate the curvature of a non-commutative Lie algebra. Further work should investigate how to improve the computation of rotation angles $\theta := \omega \Delta_t \in \mathbb{R}^{n(n-1)/2}$, that clearly has an impact on final performances.

This section covers a non exhaustive list of possibilities that our formalism offers, even though future research should help to understand the ideal tradeoff between inference speed and models expressivity.

10.5 Attention maps

To give a visual intuition of the increased recall of *MapEM*-s models, we plot in fig 8 the attention maps of four models when trying to retrieve a memory at a previously visited locations (highlighted in red). As expected, RoPE's attention is noisy and the model never manages to find the correct memory. Models who's attention rely on both structure and observation, like *MapWM* and *MapEM*-os manage to find the appropriate memory, but their attention map is not as sparse as the one where position alone is used, showing that structural attention A_P acts as an attention mask to ignore structurally irrelevant tokens. Since positions vary smoothly from one token to the next, so should their features p_t , explaining why the attention values for the *MapEM*-s model are rarely above 0.5, but can still differentiate tokens efficiently. Note that note all positions on the grid have an observation, explaining why certain positions have a high similarity (looped made by the model) but no red dot on them since there's no recall to be made.

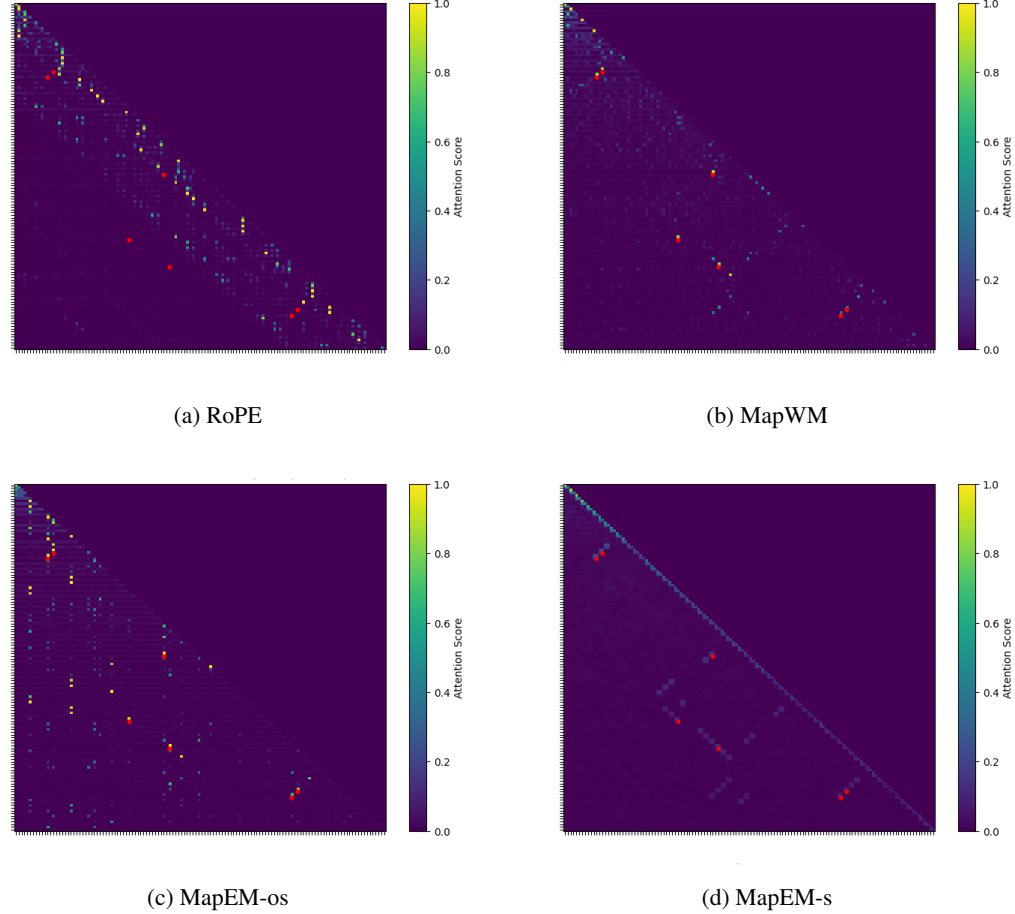


Figure 8: **MapFormers learn sparse attention maps.** RoPE / WM / EM attention maps. Red dots designate objects at previously visited location. (a) RoPE fails to attend to the correct token. (b-c) MapWM and MapEM-os models manage to attend to the relevant token but (d) MapEM-s exhibits a sparse attention map as it only needs to focus on abstract position p_t , while keys and queries can repeat an increase the similarity of structurally distinct tokens